Formulation Design & Evaluation of Methoxy PEG-PCL Micelles

5.1 MATERIALS

ETO was a kind gift from Cipla Ltd, Mumbai. Acetone, acetonitrile and sodium chloride of AR grade were purchased from S.D. Fine-chem Ltd, Mumbai. Pyrene was purchased from Sigma Aldrich, Mumbai. Bovine serum albumin (BSA) was procured from Himedia Lab., Mumbai. Drabkin's Reagent was acquired from Monozyme India Ltd., Secundrabad. Sodium hydroxide (NaOH) and hydrochloric acid (HCl) were bought from Loba Chemie Ltd., Mumbai. Iodine (I_2) and potassium iodide (KI) were purchased from Spectrochem Ltd, Mumbai.

Formulation code with respect to block copolymer used

Formulation Code	Block copolymer used
MPCL220	BCP 2-2 [MPEG(2000)-PCL (2000)]
MPCL235	BCP 2-3.5 [MPEG(2000)-PCL (3500)]
MPCL250	BCP 2-5 [MPEG(2000)-PCL (5000)]
MPCL550	BCP 5-5 [MPEG(5000)-PCL (5000)]
MPCL570	BCP5-7 [MPEG(5000)-PCL (7000)]
MPCL5100	BCP 5-10 [MPEG(5000)-PCL (10000)]

5.2 PREPARATION OF ETO LOADED MPEG-PCL (MPCL) MICELLES

A co-solvent evaporation/ nanoprecipitation method was used for the self assembly of MPEG-PCL block copolymers loaded with ETO as reported earlier with slight modification (Aliabadi et al., 2005; Zhang et al., 2004). Briefly, di-block copolymer MPEG-PCL (30 mg) and ETO (2 mg) were dissolved in 3 ml of organic solvent (acetonitrile/ acetone) and added dropwise into 5 ml of distilled water under stirring using magnetic stirrer and stirring was continued at room temperature till evaporation of organic solvent. Residual amount of solvent was removed using rotary vacuum evaporator. The resulted bluish aqueous dispersion was filtered though 0.45 micron filter membrane to remove non-incorporated drug particles and copolymer aggregates.

Initially, the effect of type of organic solvent, stirring speed and rate of addition of organic solvent to aqueous medium was optimized in terms of carrier size and encapsulation efficiency. Afterward, effects of various formulation parameters like

ratio of drug to polymer and ratio of aqueous to organic phase on particle size and percent drug entrapment was assessed. Maximum percent drug loading possible with definite amount of polymer along with their effect on particle size and polydispersity index was also estimated.

5.3 EVALUATION OF MPCL MICELLES

5.3.1 Particle size and zeta potential

Particle size and zeta potential of micelle samples were determined by dynamic light scattering method, using Zetasizer, Nano-ZS (Malvern Inst.,U.K.). Sample was filled in the cuvvette and the average volume-mean particle size and zeta potential was recorded after performing the experiments in triplicate.

5.3.2 Determination of percent entrapment efficiency and percent drug loading

The entrapment efficiency of ETO in MPCL micelles were determined by UV-visible spectrophotometer (UV 1700, PharmaSpec, Shimadzu Japan). An aliquot of micellar formulation was dissolved in acetonitrile and the amount of ETO was determined at λ max 284 nm by UV spectroscopy. The percent drug entrapment and percent drug loading were calculated using following equations.

$$\% \text{ Drug entrapment} = \frac{\text{Amount of ETO in micelles}}{\text{Amount of ETO added}} \text{ X } 100$$

$$\% \text{ Drug loading} = \frac{\text{Amount of ETO in micelles}}{\text{Amount of ETO loaded micelles}} \text{ X } 100$$

$$= \text{ ETO/ (ETO + Polymer) X } 100$$

5.3.3 Critical micelle concentration

Critical micelles concentration (CMC) is an important parameter above which an amphiphilic copolymer forms core-shell structured micelles. The CMC values of synthesized block copolymers were estimated by fluorescence spectroscopy using pyrene as fluorescent probe as reported previously (Choi et al., 2006; Kim et al., 2005). Fluorescence spectra were recorded by spectrofluorophotometer (RF-540, Shimadzu Corporation Japan) at room temperature. A known amount of pyrene was dissolved in acetone and added to a series of 20 ml vials and acetone was evaporated under nitrogen. The final concentration of pyrene in MPCL micellar solution was kept

6 X 10^{-7} M. A 10 ml of various concentration of MPCL micellar solution was added to each vial and was kept at 65 °C for 2 h and cooled to room temperature overnight to equilibrate. Polymer concentration was used in range of 1 x 10^{-4} to 2.0 mg/ml. The excitation spectra were recorded between 300 to 400 nm with an emission wavelength of 390 nm. The intensity ratios of I_{338} to I_{335} were plotted as a function of logarithm of polymer concentration. The CMC value was obtained from the intersection of the tangent to the curve at the inflection with the horizontal tangent through the points at low concentration.

5.3.4 Fixed aqueous layer thickness

The FALT of the micelles was calculated according to Gouy-Chapmann theory (Shi et al., 2005). According to this theory, zeta potential Ψ[L] as the electrostatic potential at the position of the slipping plane L (nm) is expressed as:

$$\ln \Psi[L] = \ln A - kL$$

where A is regarded as a constant, k is the Debye-Huckel parameter, equal to $\sqrt{c/03}$ (c is the molality of electrolytes) for universal salts and L gives the position of the slipping plane or thickness of the fixed aqueous layer in nanometer units. Briefly, to 1 ml of ETO loaded and placebo MPCL micelles, required amount of NaCl solution was added to make final concentration of NaCl to 25 mM, 50 mM, 75 mM and 100 mM. After 30 min of incubation at room temperature, their zeta potential was measured by Zetasizer, Nano-ZS (Malvern Inst., U.K.). The natural logarithm of zeta potential were plotted against k as per above equation and the slope obtained represents the FALT of micelles.

5.3.5 *In vitro* stability study

Interactions with serum protein have been demonstrated to be one of the key factors that influence the *in vivo* fate of systemic drug delivery vehicles such as liposomes (Patel & Moghimi 1998; Allen et al., 2002) and nanoparticles (Moghimi et al., 2003). The stability of ETO loaded and placebo MPCL micelles were evaluated in both the absence and presence of physiologically relevant concentrations of bovine serum albumin (BSA) (Liu et al., 2005). Specifically, the micelle solutions were mixed with equal volumes of PBS pH 7.4 in the absence and presence of BSA (45 g/L) and incubated at 37 °C. At various time points, 1 ml of samples were removed and

analyzed by DLS for size measurement using Zetasizer, Nano-ZS (Malvern Inst., U.K.).

5.3.6 Hemolysis study

Hemolytic activity of ETO loaded MPCL micelle was investigated to find out the percent hemolysis of formulation as reported earlier with minor changes (Shaui et al., 2004a; Letchford et al., 2009). One Sprague-Dawley rat was killed by isoflurane and blood was obtained by cardiac puncture. The blood collected in EDTA Sodium containing tubes, was centrifuged at 1500 rpm for 15 min at 4 °C. The supernatant was discarded and the pellet containing erythrocytes was washed three times with cold PBS (pH 7.4) to remove debris and serum protein by centrifugation at 1500 rpm for 15 min at 4 °C. After washing, an erythrocyte stock dispersion with fixed concentration of hemoglobin was prepared with buffer (3 parts centrifuged erythrocytes plus 11 parts of PBS). The stock dispersion was stored at 2- 8° C for maximum 24 h and its stability was checked by photometric monitoring. (100 µl in 0.9 ml of buffer solution).

A 100 µl of aliquot of erythrocytes dispersion was added to 900 µl of MPCL micelles (prepared in PBS) containing different amount of ETO. ETO injection and placebo batch of injection was also prepared according to marketed formulation and evaluated for hemolysis studies to find out the effect of drug, surfactant and other excipients on erythrocyte lysis. Samples were incubated at 37 °C for various time periods in shaking water bath at low speed. After incubation, debris and intact erythrocytes were removed by centrifugation at 1500 rpm for 10 min. A 100 µl of supernatant was added to 3 ml of Drabkin's Reagent at room temp and kept for five min. Absorbance's of samples were measured at 540 nm by UV-visible spectrophotometer (UV 1700, PharmaSpec, Shimadzu Japan) using Drabkin's Reagent as blank. Complete hemolysis was achieved using 2% Triton X-100, yielding the 100 % control value. Zero percent hemolysis was considered as PBS buffer-treated erythrocyte solution (control). The percent hemolysis was calculated using following equation.

$$\% \text{ Hemolysis} = \frac{\text{Abs Sample} - \text{Abs Control}}{\text{Abs Triton X-100} - \text{Abs Control}} \times 100$$

5.3.7 PEG surface density

PEG surface density of nanoparticles plays a vital role in the *invitro* and *in vivo* performance of nanoparticles. PEG surface density of MPCL micelles of various block length were determined using method described earlier (Shai et al., 2005; Paracchia et al., 1997). Both ETO loaded and placebo batches of various MPCL micelles were prepared and diluted with distilled water. To 5 ml of diluted dispersion, 2 ml of 2 N NaOH added and kept for five days at 50 °C. Then samples were neutralized with 1 N HCl to pH 7.0 and final volume was made upto 10 ml. A 250 µl of I_2/KI solution (I_2 10g/l and KI 20 g/l) was added and samples were mixed well and absorbance was measured at 525 nm by UV-visible spectrophotometer (UV 1700, PharmaSpec, Shimadzu Japan). The total amount of PEG after micelle degradation was calculated based on standard calibration curve of PEG (Chapter 3.2). Fraction of PEG was calculated based on the amount of PEG obtained divided by total amount of PEG-PCL polymer used in formulation.

PEG surface density was calculated based on equation

$$\delta = \frac{N \times d \times \alpha \times r}{3MwPEG}$$

where δ is the surface density of PEG chains (PEG/nm^2), N is the Avogadro number 6.021 x 10^{23}/ mole, r is the particle radius neglecting the PEG layer thickness (error <10%), d is the density of micelles, α is the fraction of PEG content after micelles degradation and MwPEG stands for molecular weight of PEG. From the data of surface density of PEG chains, the average distance D between two neighboring PEG was calculated based on the following equation.

$$D = \sqrt{1/\delta}$$

5.4 RESULT AND DISCUSSION

5.4.1 Preparation of MPCL micelles

Method of preparation of aqueous solutions of amphiphilic block copolymers has a great impact on the particle size, size distribution and stability of nanoparticles formed (Vangeyte et al., 2004). Very few studies has been carried out using low molecular hydrophobic content amphiphilic copolymers and poly(ethylene oxide)-b-poly(propylene oxide)-b-poly(ethylene oxide) copolymers, known as "pluronics" (Tanodekaew et al., 1997) by direct solubilization method. However, this method is suitable for polymers with lower molecular weight hydrophobic part and higher molecular weight of hydrophilic part. Incase of lower water solubility of copolymers, indirect methods of dissolution is required, which need the temporary use of a common organic solvent miscible with water. Zhang et al. (1998) proposed two methods for the preparation of "crew-cut" micelles: (i) dropwise addition of water to the organic solution until aggregation occurs, (ii) preparation of a micellar solution in an appropriate organic solvent/water mixture, followed by addition of a large amount of water in order to freeze the micelles, and by dialysis against pure water. Precipitation or emulsification by addition of the copolymer organic solution into water (under stirring or not) is widely used method (Gan et al., 1999). Dialysis of an organic solution against water or water/organic solvent mixtures of increasing water content is an alternative method (Kim & Lee, 2001).

Fabrication of MPEG-PCL micelles loaded with drug has been mostly accomplished through either dialysis (Allen et al., 2000) or co-solvent evaporation methods (Jette et al., 2004; Shuai et al., 2004a,b). In the co-solvent evaporation method, the block copolymer and the drug are dissolved in a volatile, water miscible organic solvent (selective co-solvent for the core-forming block). Self assembly and drug entrapment is then prompted by the addition of organic phase to the water (non-solvent for the core forming block) followed by the evaporation of the organic co-solvent. The organic solvent content is afterward decreased by the injection of the solution in an excess of water by evaporation. The thermodynamic quality of the solvent for the hydrophobic blocks deteriorates with decreasing content of the organic solvent and the association number increases (Radek et al., 2007). A further decrease in the content of the organic solvent causes the collapse of hydrophobic cores, and the nanoparticles kinetically "freeze". Their association number does not change any

more, although it depends on the copolymer concentration, its composition and architecture, rate of the organic solvent removal, temperature, and other factors.

The co-solvent evaporation method bears several advantages over dialysis method including more feasibility for scale up and less chance for drug loss during dialysis in the encapsulation process (Vangyate et al., 2004). Moreover, it was observed that dialysis method led to the formation of large aggregates indicating a fast exchange of solvent, most likely due to the large porosity of the dialysis membrane used and reproducibility problem, making the experimental size uncertain. A comparison between individual studies by separate research groups on the self-assembly of MPEG-PCL by co-solvent evaporation method, implies that apart from block copolymer molecular weight, solvent composition in the self-association process may play a significant role in determining the final properties of the assembled structures (Jette et al., 2004; Kim et al., 1998; Shuai et al., 2004a,b).

Based on the finding of studies reported by various authors as above, a co-solvent evaporation method was chosen and two water miscible organic solvent **acetone** and **acetonitrile (ACN)** were selected for formulation of MPCL micelles. Various other organic solvent like tetrahydrofuran (THF) and dimethyl sulphoxide (DMSO) was used by Vangyate el al. (2004). They reported that higher viscosity of DMSO and lower miscibility of THF with water (in relation to a low dielectric constant compared to water and the other organic solvents) might slow down the mixing rate which resulted in to larger size particles. Nanoprecipitation or co-solvent evaporation method can be performed by either addition of organic solution of polymer in to water dropwise or reverse. Although, the intrinsically low precipitation rate is expected to be increased when the organic solution is added to a large amount of water compared to the reverse addition i.e. water to the organic phase. As a result, smaller particles are formed upon addition of the organic solution in water (Vangyate et al., 2004).

Formulation Code	Organic Solvent			
	Acetone		ACN	
	Particle size (nm)	PDE	Particle Size (nm)	PDE
MPCL220	36.24 ± 5.88	51.67 ± 3.68	40.77 ± 2.09	50.89 ± 2.53
MPCL235	40.79 ± 2.89	59.04 ± 3.01	45.32 ± 4.98	60.20 ± 2.65
MPCL250	63.04 ± 3.29	76.34 ± 6.77	68.70 ± 4.07	76.71 ± 3.37
MPCL550	73.35 ± 3.71	79.28 ± 3.91	77.09 ± 4.80	78.89 ± 4.11
MPCL570	76.93 ± 4.68	80.81 ± 4.97	83.41 ± 3.74	80.08 ± 3.90
MPCL5100	82.85 ± 2.61	83.12 ± 2.93	92.76 ± 3.32	83.78 ± 3.62

Table 5.1 Effect of different organic solvent on particle size and percent drug entrapment of MPCL micelles (Results are mean ± S. D. and n=3)

As shown in Table 5.1, there was no any significant difference found in percent drug entrapment (PDE) for both the organic solvents but an increase in particle size from 5 to 10 nm was observed with the use of ACN compared to acetone. The effect of organic solvent on particle size of MPCL micelles was evaluated by Aliabadi et al. (2007) and it was found that use of acetone and THF increased particle size upto 5 nm and 25 nm respectively compared ACN. However in present studies, contradictory results were observed and the probable reason behind these might be due to longer time required for complete evaporation of ACN. It is noteworthy that acetone: water system may be beneficial in terms of scale-up because of a lower boiling point and is safe to use in drug delivery compared to ACN based on health rating.

It was reported that both controlled addition rate of one phase into the other one and the stirring rate are important to maintain constant particle size with good reproducibility (Vangyate et al., 2004). In order to evaluate the effect of speed on particle size and drug encapsulation, stirring speed was kept at three different level i.e. 500, 1000 and 1500 rpm. As shown in Table 5.2 & Figure 5.1, it was observed that the stirring speed of 1500 rpm resulted in increase in particle size upto 8 to 24 nm with significant reduction in drug entrapment compared to stirring rate of 1000 rpm. At the same time, at lower stirring speed (500 rpm), an increase in particle size upto 6 to 10 nm with no any significant reduction in drug entrapment was observed. Increase in particle size observed at 1500 rpm might be attributed to higher collision and aggregation effect free drug present in the system.

Formulation Code	Stirring speed (rpm)					
	500		1000		1500	
	Particle size (nm)	PDE	Particle size (nm)	PDE	Particle size (nm)	PDE
MPCL220	42.55 ± 3.16	50.99 ± 4.30	36.24 ± 5.88	51.67 ± 3.68	60.87 ± 9.43	40.43 ± 5.11
MPCL235	45.38 ± 2.45	59.29 ± 4.22	40.79 ± 2.89	59.04 ± 3.01	66.98 ± 7.71	46.55 ± 4.08
MPCL250	69.79 ± 3.74	77.06 ± 4.40	63.04 ± 3.29	76.34 ± 6.77	86.76 ± 6.49	60.87 ± 3.45
MPCL550	80.04 ± 3.45	78.90 ± 3.83	73.35 ± 3.71	79.28 ± 3.91	82.34 ± 9.35	66.05 ± 6.32
MPCL570	86.65 ± 5.02	83.07 ± 3.08	76.93 ± 4.68	80.81 ± 4.97	89.11 ± 8.28	73.02 ± 4.63
MPCL5100	91.35 ± 4.30	81.65 ± 3.05	82.85 ± 2.61	83.12 ± 2.93	98.04 ± 7.53	74.34 ± 5.24

Table 5.2 Effect of stirring speed on particle size and percent drug entrapment of MPCL micelles (Results are mean ± S. D. and n=3)

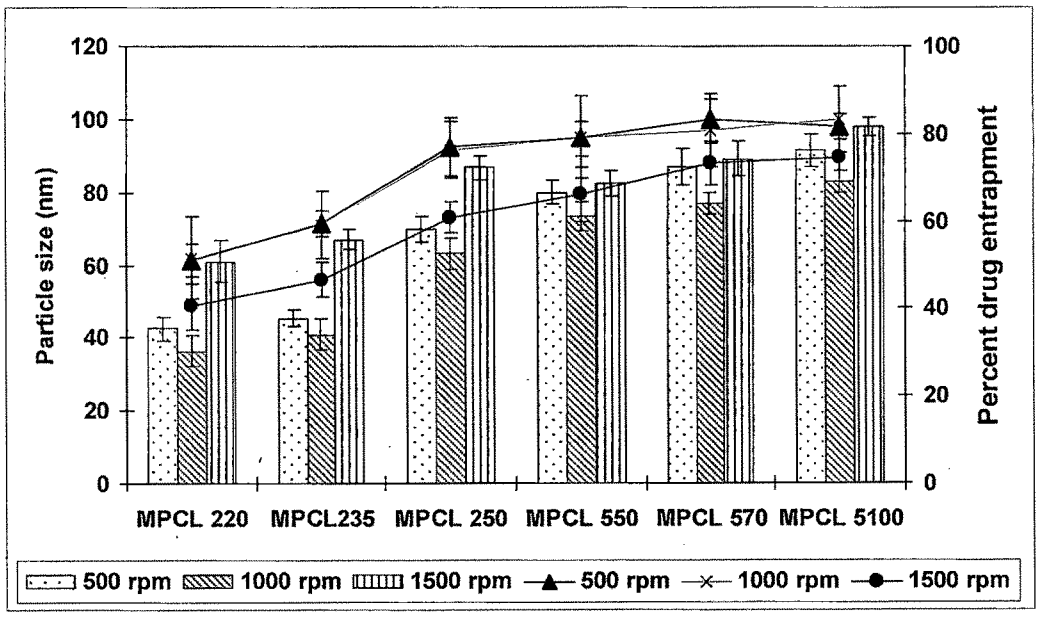

Figure 5.1 Effect of stirring speed on particle size and percent drug entrapment of MPCL micelles (Results are mean ± S. D. and n=3)

Rate of addition of organic solvent to aqueous phase was evaluated at three different level i.e. 0.5, 1.0 and 1.5 ml/min. As shown in Table 5.3 & Figure 5.2, at 0.5 and 1.0 ml/min rate of addition, there was no any increase in particle size observed. But if the rate increased to 1.5 ml/min, a drastic increase in particle size with reduction in drug entrapment observed. It was believed that at 1.5 ml/min addition rate, the drug might diffuse rapidly to aqueous phase without entrapping into micelle, which may

hampered the stability and drug loading efficiency of system. The results obtained are in same fashion as it was observed with different rate of stirring.

Formulation Code	Rate of addition of solvent (ml/min)					
	0.5		1.0		1.5	
	Particle size (nm)	PDE	Particle size (nm)	PDE	Particle size (nm)	PDE
MPCL220	36.22 ± 2.90	50.97 ± 3.09	36.24 ± 5.88	51.67 ± 3.68	61.33 ± 6.08	40.82± 4.31
MPCL235	40.85 ± 3.83	59.22 ± 2.08	40.79 ± 2.89	59.04 ± 3.01	69.76± 3.12	50.17± 4.88
MPCL250	62.79 ± 2.51	76.03 ± 4.60	63.04 ± 3.29	76.34 ± 6.77	88.39± 3.61	55.34± 3.23
MPCL550	74.02 ± 4.88	79.55 ± 3.13	65.35 ± 3.71	79.28 ± 3.91	97.76± 4.89	63.01± 5.98
MPCL570	76.98 ± 2.71	79.67 ± 4.04	76.93 ± 4.68	80.81 ± 4.97	100.61± 6.08	66.95± 4.29
MPCL5100	84.11 ± 4.22	82.92 ± 3.71	82.85 ± 2.61	83.12 ± 2.93	115.22± 5.29	72.21± 5.34

Table 5.3 Effect of rate of addition of organic solvent to aqueous phase on particle size and drug entrapment of MPCL micelles (Results are mean ± S. D. and n=3).

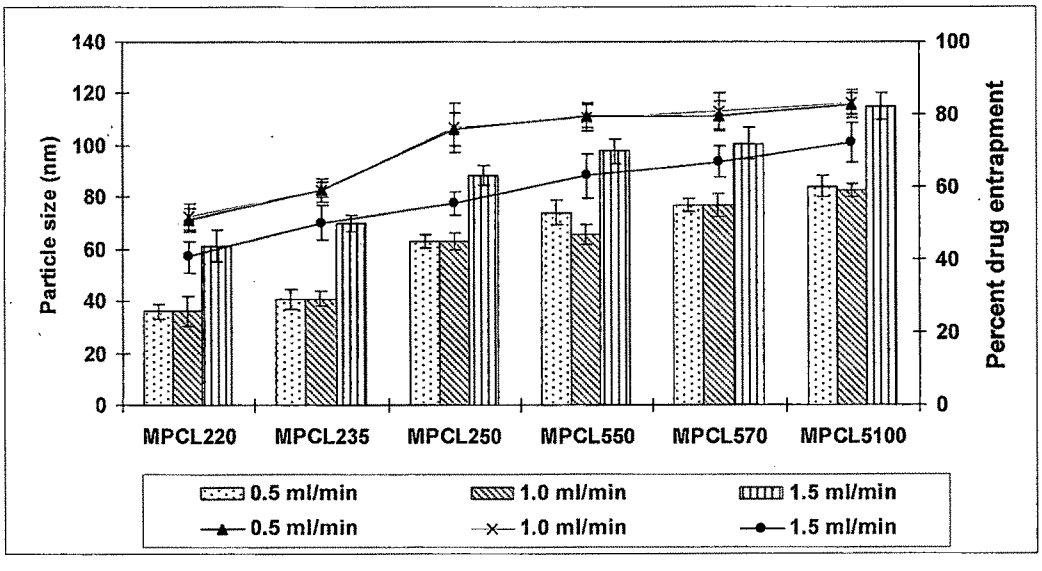

Figure 5.2 Effect of rate of addition of organic solvent to aqueous phase on particle size and drug entrapment of MPCL micelles (Results are mean ± S. D. and n=3)

Influence of formulation parameters on particle size and percent drug entrapment was evaluated by varying drug to polymer ratio and aqueous phase to organic phase. Table 5.4 to 5.7 shows the effect of formulation parameter on particle size and percent drug entrapment. It was observed that both particle size and percent drug entrapment increased with increase in the ratio of drug to polymer. Moreover, an increase in particle size and drug entrapment was also observed with increase in molecular weight of hydrophobic part of all different block length copolymer. The increase in the block length of PCL resulted in a larger core diameter, so more drug molecules can be incorporated.

The reason for this is that as the PCL block length increases, the aggregation number of the micelle increases, resulting in a larger core, which allows a higher loading efficiency of drug. The results obtained are in accordance with Gadelle et al. (1995). Similarly, Kozlov et al. (2000) showed that an increase in the PCL block length also increased the partition coefficient which is a convenient way to express the affinity of the drug for the micelle core or for the external environment. It was found that MPCL220, MPCL235 and MPCL250 micelles at drug to polymer ratio of 1:20 resulted in to particle size of 36.57 ± 3.16, 39.52 ± 3.18 nm & 61.22 ± 1.98 nm with and percent drug entrapment of 61.44 ± 5.10, 82.50 ± 4.86 & 89.07 ± 3.89 respectively (Table 5.4 & Figure 5.3). Micellar formulations MPCL550, MPCL570 and MPCL5100 exhibited particle size of 68.35 ± 4.18, 78.31 ± 2.14 & 86.97 ± 3.01 nm with 88.79 ± 4.34, 91.07 ± 3.18 & 95.92 ± 3.76 percent drug entrapment at drug to polymer ratio of 1:20 (Table 5.5 & Figure 5.4). A minor difference in particle size of MPCL220 and MPCL235 micelles was observed, which might be attributed to limitation of co-solvent method employed in case of MPCL220 micelles (Soppimath et al., 2001). This result signifies that the drug encapsulation efficiency depends on the copolymer composition as well as the ratio of ETO to polymer.

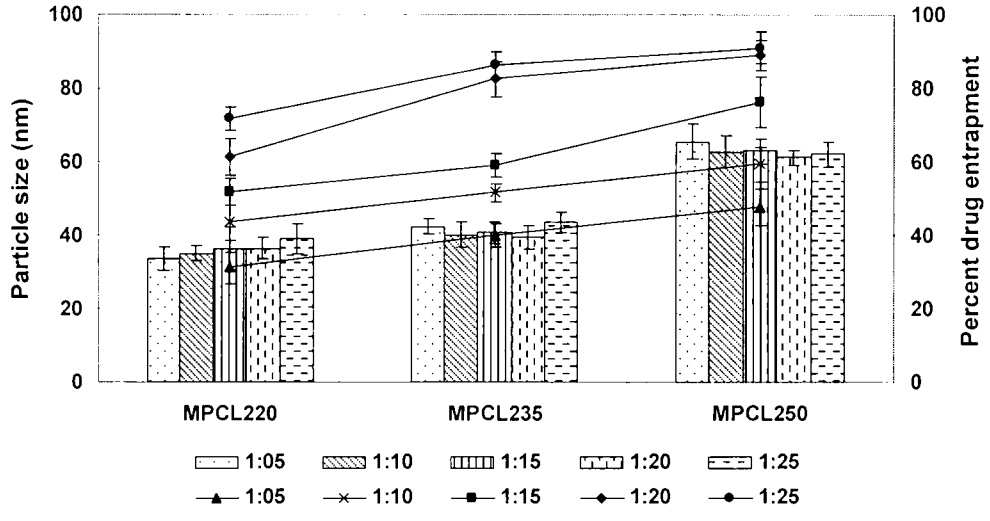

Figure 5.3 Influence of ratio of drug to polymer on particle size and percent drug entrapment of MPCL220, MPCL235 and MPCL250 micelles (Results are mean ± S. D. and n=3)

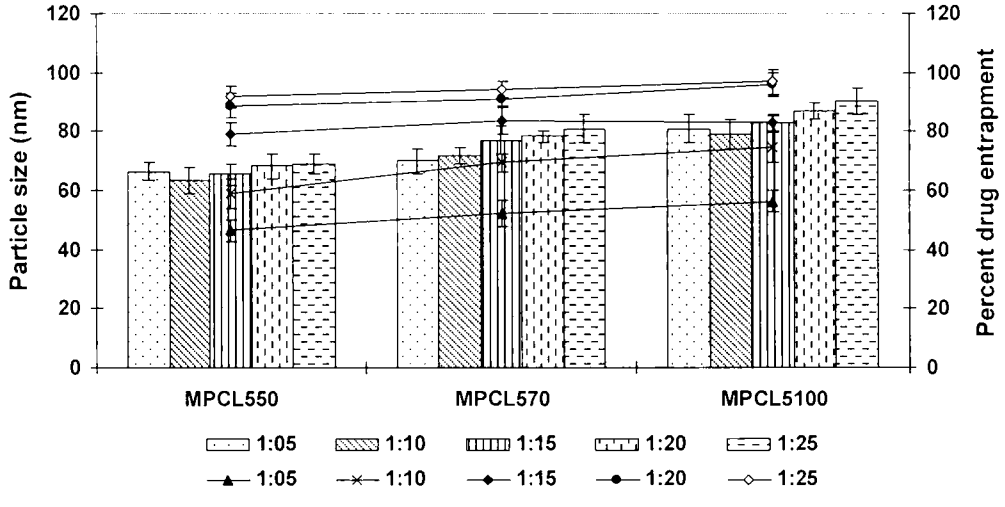

Figure 5.4 Influence of ratio of drug to polymer on particle size and percent drug entrapment of MPCL550, MPCL570 and MPCL5100 micelles (Results are mean ± S. D. and n=3)

Ratio of drug to polymer (mg)	MPCL220			MPCL235			MPCL250		
	P. Size (nm)	PDI	PDE	P. Size (nm)	PDI	PDE	P. Size (nm)	PDI	PDE
1:5	33.53 ± 3.08	0.236 ± 0.076	31.18 ± 4.36	42.38 ± 2.04	0.152 ± 0.028	39.89 ± 3.08	65.64 ± 4.72	0.181 ± 0.043	47.76 ± 5.18
1:10	35.09 ± 2.08	0.252 ± 0.069	43.55 ± 4.71	40.18 ± 3.56	0.167 ± 0.035	51.76 ± 2.54	62.89 ± 4.16	0.178 ± 0.023	59.32 ± 4.90
1:15	36.24 ± 5.88	0.250 ± 0.038	51.67 ± 3.68	40.79 ± 2.89	0.179 ± 0.030	59.04 ± 3.01	63.04 ± 3.29	0.189 ± 0.039	76.34 ± 6.77
1:20	36.57 ± 3.16	0.268 ± 0.029	61.44 ± 5.10	**39.52 ± 3.18**	**0.156 ± 0.024**	**82.50 ± 4.86**	**61.22 ± 1.98**	**0.183 ± 0.026**	**89.07 ± 3.89**
1:25	**39.02 ± 4.23**	**0.245 ± 0.063**	**71.97 ± 3.15**	43.69 ± 2.76	0.162 ± 0.026	86.44 ± 3.56	62.14 ± 3.38	0.169 ± 0.027	91.02 ± 4.23

Table 5.4 Influence of ratio of drug to polymer on particle size and percent drug entrapment of MPCL220, MPCL235 and MPCL250 micelles (Results are mean ± S. D. and n=3)

Ratio of drug to polymer (mg)	MPCL550			MPCL570			MPCL5100		
	P. Size (nm)	PDI	PDE	P. Size (nm)	PDI	PDE	P. Size (nm)	PDI	PDE
1:5	66.38 ± 2.96	0.217 ± 0.035	46.38 ± 3.76	69.82 ± 4.42	0.223 ± 0.045	52.23 ± 4.57	80.97 ± 4.67	0.235± 0.039	56.18 ± 3.58
1:10	63.37 ± 4.58	0.226 ± 0.021	58.76 ± 5.06	72.04 ± 2.80	0.212 ± 0.026	69.34 ± 3.03	79.04 ± 5.18	0.193 ± 0.020	74.60 ± 5.02
1:15	65.35 ± 3.71	0.201 ± 0.037	79.28 ± 3.91	76.93 ± 4.68	0.201 ± 0.028	80.81 ± 4.97	**82.85 ± 2.61**	**0.178 ± 0.018**	**83.12 ± 2.93**
1:20	**68.35 ± 4.18**	**0.180 ± 0.022**	**88.79 ± 4.34**	**78.31 ± 2.14**	**0.182 ± 0.030**	**91.07 ± 3.18**	86.97 ± 3.01	0.185 ± 0.030	95.92 ± 3.76
1:25	68.95 ± 3.16	0.194 ± 0.020	91.76 ± 3.83	80.87 ± 4.72	0.189 ± 0.022	93.98 ± 2.76	90.29 ± 4.45	0.196 ± 0.025	96.84 ± 4.06

Table 5.5 Influence of ratio of drug to polymer on particle size and percent drug entrapment of MPCL550, MPCL570 and MPCL5100 micelles (Results are mean ± S. D. and n=3)

Ratio of aqueous to organic phase (ml)	MPCL220			MPCL235			MPCL250		
	P. Size (nm)	PDI	PDE	P. Size (nm)	PDI	PDE	P. Size (nm)	PDI	PDE
1:0.2	45.21 ± 3.03	0.303 ± 0.041	68.23.± 3.18	48.66 ± 2.89	0.206 ± 0.028	78.92 ± 3.83	64.09 ± 5.63	0.233 ± 0.050	86.24 ± 4.09
1:0.4	39.02 ± 4.23	0.245 ± 0.063	71.97 ± 3.15	39.52 ± 3.18	0.156 ± 0.024	82.50 ± 4.86	61.22 ± 1.98	0.183 ± 0.026	89.07 ± 3.89
1:0.6	**38.23 ± 4.73**	**0.213 ± 0.054**	**70.34 ± 3.86**	**38.53 ± 2.53**	**0.152 ± 0.026**	**81.18 ± 2.03**	**52.90 ± 2.28**	**0.164 ± 0.030**	**88.76 ± 2.18**
1:0.8	53.18 ± 4.28	0.308 ± 0.058	72.67 ± 5.19	40.73 ± 3.02	0.182 ± 0.027	80.89 ± 3.61	56.20 ± 2.36	0.191 ± 0.023	86.94 ± 4.76
1:1	57.53 ± 3.89	0.376 ± 0.046	69.29 ± 4.05	45.91 ± 4.53	0.225 ± 0.045	80.38 ± 4.18	58.61 ± 6.53	0.242 ± 0.057	85.28 ± 5.08

Table 5.6 Influence of ratio of aqueous to organic phase on particle size and percent drug entrapment of MPCL220, MPCL235 and MPCL250 micelles (Results are mean ± S. D. and n=3)

Ratio of aqueous to organic phase (ml)	MPCL550			MPCL570			MPCL5100		
	P. Size (nm)	PDI	PDE	P. Size (nm)	PDI	PDE	P. Size (nm)	PDI	PDE
1:0.2	76.46 ± 6.54	0.209 ± 0.024	84.18 ± 3.10	87.44 ± 5.67	0.201 ± 0.041	89.07 ± 3.03	103.30 ± 4.06	0.215 ± 0.029	82.53 ± 4.37
1:0.4	68.35 ± 4.18	0.180 ± 0.022	88.79 ± 4.34	78.31 ± 2.14	0.182 ± 0.030	91.07 ± 3.18	82.85 ± 2.61	0.178 ± 0.018	83.12 ± 2.93
1:0.6	**67.89 ± 3.08**	**0.159 ± 0.022**	**88.51 ± 3.20**	75.74 ± 2.87	0.164 ± 0.026	91.37 ± 2.68	79.91 ± 3.86	0.157 ± 0.023	83.89 ± 1.73
1:0.8	72.89 ± 4.31	0.174 ± 0.030	86.89 ± 5.08	**73.39 ± 4.08**	**0.143 ± 0.019**	**92.06 ± 3.48**	**76.25 ± 2.69**	**0.136 ± 0.031**	**82.78 ± 3.60**
1:1	74.32 ± 6.17	0.205 ± 0.033	87.41 ± 3.82	76.98 ± 3.70	0.165 ± 0.031	89.89 ± 3.37	81.71 ± 3.18	0.146 ± 0.018	83.16 ± 4.69

Table 5.7 Influence of ratio of aqueous to organic phase on particle size and percent drug entrapment of MPCL550, MPCL570 and MPCL5100 micelles (Results are mean ± S. D. and n=3)

A review of individual data from separate research works points to the influence of solvent/co-solvent composition on the properties of MPCL micelles prepared by the co-solvent evaporation method (Jette et al., 2004; Shuai et al., 2004a,b). To achieve an optimum polymeric micellar carrier for the delivery of ETO, a systematic study determining the effect of solvent/co-solvent composition on carrier size and ETO encapsulation has been carried out. The ratio of aqueous to organic phase (acetone) was varied as shown in Table 5.6 & 5.7 and their effect on particle size and percent drug entrapment was studied. At ratio of aqueous to organic phase of 1:0.6, MPCL220, MPCL235 and MPCL250 micelles showed 38.23 ± 4.73, 38.53 ± 2.53 & 52.90 ± 2.28 nm particle size with PDI 0.213, 0.152, 0.164 respectively (Table 5.6 & Figure 5.5). In MPCL550 micelles, at ratio aqueous to organic phase of 1:0.6, a lowest particle size of 67.89 ± 3.08 nm with PDI 0.159 was found while MPCL570 and MPCL5100 at 1:0.8 ratio of aqueous to organic phase exhibited particle size of 73.39 ± 4.08 and 76.25 ± 2.69 nm with PDI 0.143 and 0.136 respectively (Table 5.7 and Figure 5.6). Despite change in particle size and PDI, a small change in drug entrapment was observed in all micellar formulation at various aqueous to organic phase ratios.

It was observed that polymer concentration in organic solvent affected much on particle size and PDI. It was found that particle size and PDI of the MPCL micelles decreased with decrease in polymer concentration upto certain point and again increased with further decrease in polymer concentration. It was due to lower copolymer concentration resulted in to higher diffusion of the organic phase into aqueous phase, which may result in a greater polydispersity index and larger particle size of each nanoparticle which was observed by Vangeyte et al. (2004). At the same time at high aqueous to organic phase ratio, complete evaporation of solvent takes time and resulted into higher PDI with broader particle size distribution. The results obtained here indicates that particle size adjustment could be attained by deliberately using different copolymers or simply via variation of the copolymer concentration in organic phase, which endows these drug delivery carriers with fine flexibility in terms of size control. Johnson and Prud'homme (2003 a,b) observed that a higher polymer concentration in the organic phase can decrease the aggregation time of micellization and lead to the formation of more compact nanoparticles.

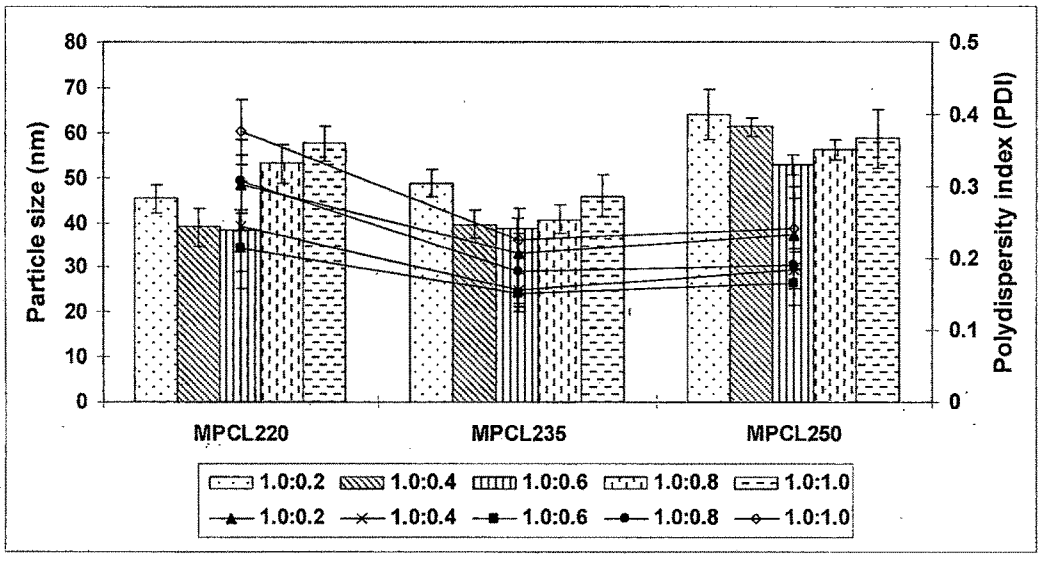

Figure 5.5 Influence of ratio of aqueous to organic phase on particle size and percent drug entrapment of MPCL220, MPCL235 and MPCL250 micelles (Results are mean ± S. D. and n=3)

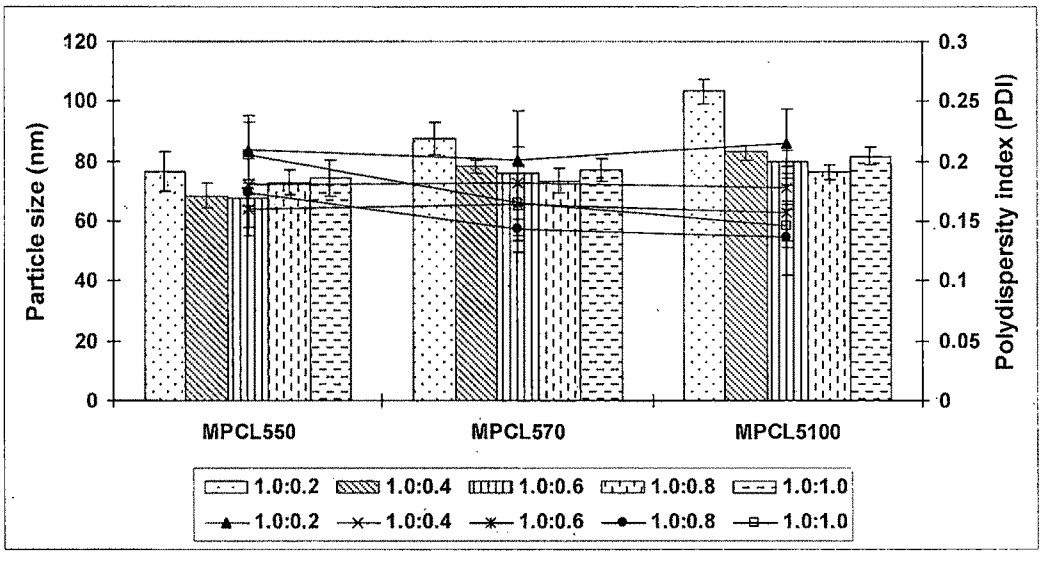

Figure 5.6 Influence of ratio of aqueous to organic phase on particle size and percent drug entrapment of MPCL550, MPCL570 and MPCL5100 micelles (Results are mean ± S. D. and n=3)

Formulation Code	Theoretical Percent drug loading	Practical percent drug loading obtained	PDE	Particle size (nm)	PDI
MPCL220	2.00	1.72 ± 0.11	87.81 ± 5.76	37.84 ± 2.90	0.215 ± 0.035
	3.00	2.35 ± 0.15	80.23 ± 5.08	38.03 ± 3.19	0.206 ± 0.041
	4.00	**2.73 ± 0.15**	**70.34 ± 3.86**	**38.23 ± 4.73**	**0.213 ± 0.054**
	5.00	2.69 ± 0.19	54.27 ± 4.93	43.09 ± 3.73	0.310 ± 0.060
	6.00	2.42 ± 0.33	40.53 ± 6.63	43.50 ± 0.044	0.329 ± 0.044
MPCL235	2.50	2.22 ± 0.09	91.92 ± 3.98	37.39 ± 2.08	0.148 ± 0.028
	3.75	3.18 ± 0.11	87.80 ± 3.17	37.84 ± 2.67	0.155 ± 0.031
	5.00	**3.90 ± 0.10**	**81.18 ± 2.03**	**38.53 ± 2.53**	**0.152 ± 0.026**
	6.25	3.91 ± 0.25	65.16 ± 4.10	42.62 ± 1.89	0.183 ± 0.032
	7.50	3.48 ± 0.54	48.12 ± 7.33	49.84 ± 4.70	0.194 ± 0.028
MPCL 250	2.50	2.46 ± 0.04	98.92 ± 1.87	54.71 ± 4.45	0.154 ± 0.034
	3.75	3.47 ± 0.13	93.27 ± 3.61	54.12 ± 3.60	0.161 ± 0.026
	5.00	**4.24 ± 0.11**	**88.76 ± 2.28**	**52.90 ± 1.98**	**0.164 ± 0.030**
	6.25	4.22 ± 0.29	70.57 ± 3.98	55.82 ± 2.53	0.178 ± 0.027
	7.50	4.06 ± 0.44	56.53 ± 5.91	59.21 ± 4.30	0.190 ± 0.036

Table 5.8 Percent drug loading of ETO in MPCL220, MPCL235 and MPCL250 micelles with different amount of ETO (Results are mean ± S. D. and n=3).

Formulation Code	Theoretical Percent drug loading	Practical percent drug loading obtained	PDE	Particle size (nm)	PDI
MPCL550	2.50	2.10 ± 0.09	98.33 ± 3.74	68.85 ± 4.18	0.144 ± 0.019
	3.75	3.45 ± 0.15	95.50 ± 4.12	71.15 ± 3.42	0.152 ± 0.021
	5.00	**4.23 ± 0.15**	**88.51 ± 3.20**	**67.89 ± 3.08**	**0.159 ± 0.022**
	6.25	4.19 ± 0.32	70.01 ± 5.25	68.85 ± 3.87	0.204 ± 0.030
	7.50	3.97 ± 0.36	55.23 ± 4.88	68.98 ± 5.30	0.220 ± 0.028
MPCL570	2.50	2.39 ± 0.12	97.97 ± 5.06	73.13 ± 4.01	0.136 ± 0.026
	3.75	3.49 ± 0.18	96.67 ± 4.98	73.90 ± 3.89	0.140 ± 0.030
	5.00	**4.40 ± 0.17**	**92.06 ± 3.48**	**73.39 ± 4.08**	**0.143 ± 0.019**
	6.25	4.28 ± 0.21	71.67 ± 3.39	80.08 ± 2.43	0.180 ± 0.046
	7.50	4.23 ± 0.25	59.03 ± 5.67	89.74 ± 5.08	0.234 ± 0.050
MPCL5100	3.33	3.07 ± 0.12	95.18 ± 3.61	80.54 ± 3.68	0.139 ± 0.029
	5.00	4.35 ± 0.23	91.01 ± 4.69	81.77 ± 2.76	0.128 ± 0.020
	6.66	**5.23 ± 0.24**	**82.78 ± 3.60**	**76.25 ± 2.69**	**0.136 ± 0.031**
	8.33	5.32 ± 0.41	67.46 ± 4.97	80.80 ± 2.80	0.198 ± 0.018
	10.00	5.06 ± 0.35	53.38 ± 3.55	81.28 ± 4.62	0.220 ± 0.031

Table 5.9 Percent drug loading of ETO in MPCL550, MPCL570 and MPCL5100 micelles with different amount of ETO (Results are mean ± S. D. and n=3).

The nanocarrier should ideally have maximum drug loading. However, several factors affect drug loading content and drug encapsulation efficiency of the core-shell structured nanoparticles prepared by nano-precipitation method. The major factors are the affinity of the loaded drug with the core-forming polymer, the volume of the hydrophobic core, drug solubility in water and drug–drug interaction (Allen et al., 1999). Micellar formulations of ETO were prepared by varying the amount the drug keeping other parameters constant. Table 5.8 and 5.9 represents the maximum practical drug loading achieved by various micellar formulations. MPCL220, MPCL235 and MPCL250 showed maximum drug loading of 2.73, 3.91 and 4.24 percent while MPCL550, MPCL570 and MPCL5100 showed 4.23, 4.40 and 5.32 percent drug loading. A practical drug loading obtained with different micellar formulations was solely dependent on the molecular weight of block copolymer especially the hydrophobic core part and increased with increase in hydrophobic core part molecular weight (Figure 5.7).

Moreover, a drop in percent drug loading with increase in particle size and polydispersity index was observed in all micellar formulation after saturation limit attained. The probable reason behind this might be attributed to the fact that higher drug concentration in the organic phase leads to a higher diffusion of ETO into water and hence a larger portion of the drug might move out from the organic phase without being encapsulated before the formation of the micelles. In addition, when feed concentration of drug is higher than its saturation solubility in system, the non incorporated drug may act as coagulant in system and affects the overall stability of micelles obtained in terms of particle size, percent drug loading and PDI. The results obtained are in accordance with Hu et al. (2007) & Zhang et al. (2004), they reported that beyond the saturation solubility, drug was precipitated out and nanoparticles exhibited lower drug encapsulation.

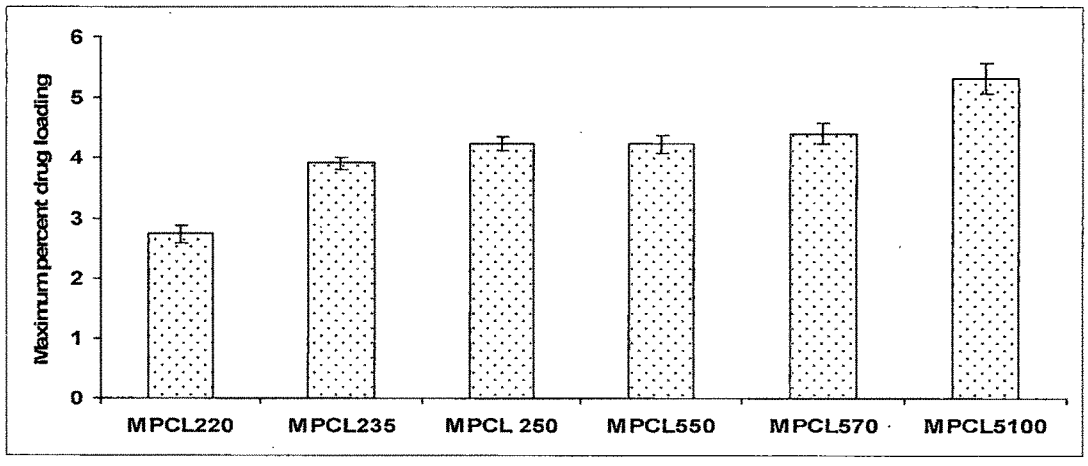

Figure 5.7 Maximum practical percent drug loading achieved in various MPCL micelles (Results are mean ± S. D. and n=3)

5.4.2 Evaluation of MPCL micelles

5.4.2.1 Particle size and zeta potential

The particle size of MPCL micelles was measured using Zetasizer, Nano-ZS (Malvern Inst., U.K.) Figure 5.8 represent a typical particle size distribution of ETO loaded MPCL235 micelles which showed monomodal peak with narrow particle size distribution.

			Diam. (nm)	% Intensity	Width (nm)
Z-Average (d.nm):	38.18	Peak 1:	42.39	98.6	16.01
PdI:	0.152	Peak 2:	4619	1.4	820.5
Intercept:	0.959	Peak 3:	0.000	0.0	0.000
Result quality :	Good				

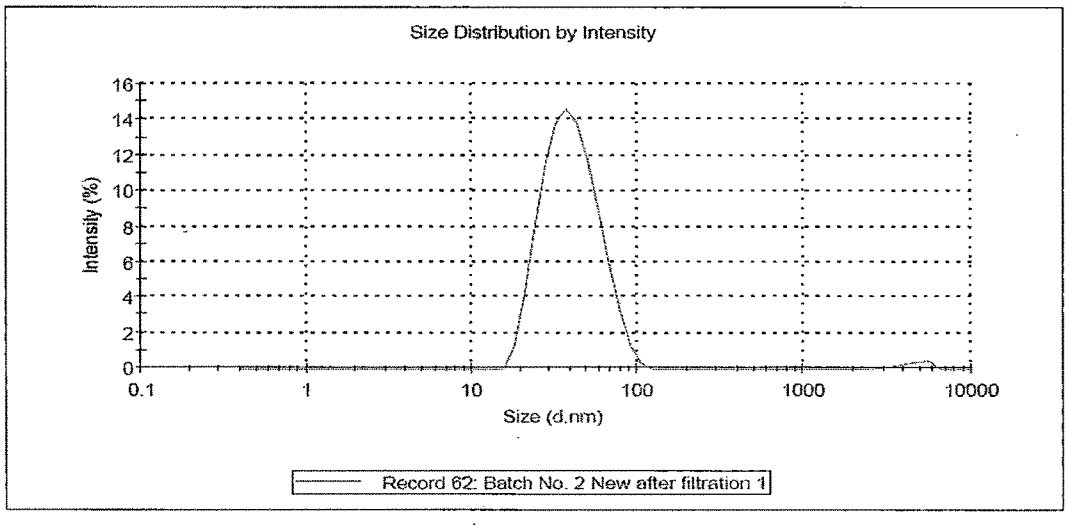

Figure 5.8 Typical particle size distributions of ETO loaded MPCL235 micelles

A high negative or positive zeta potential is required for strong repellant interaction among nanoparticles/ micelles in dispersion resulting into high stability. MPCL micelles prepared from different molecular weight block copolymer exhibited zeta potential near to neutral as reported in Table 5.10 and Figure 5.9. It is because of the PEG segment which capped the carboxyl acid end groups of the PCL chains resulted in to low negative zeta potentials as reported earlier (Hu et al., 2007). The excellent stability of these micelles in aqueous solution was due to the existence of the neutral PEG shell.

Formulation Code	Zeta potential (mV) ± S. D.
MPCL 220	-4.18 ± 0.37
MPCL 235	-4.09 ± 0.45
MPCL 250	-4.98 ± 0.33
MPCL 550	-4.16 ± 0.45
MPCL 570	-4.65 ± 0.39
MPCL 5100	-5.12 ± 0.41

Table 5.10 Average zeta potential of MPCL micellar formulation (n=3)

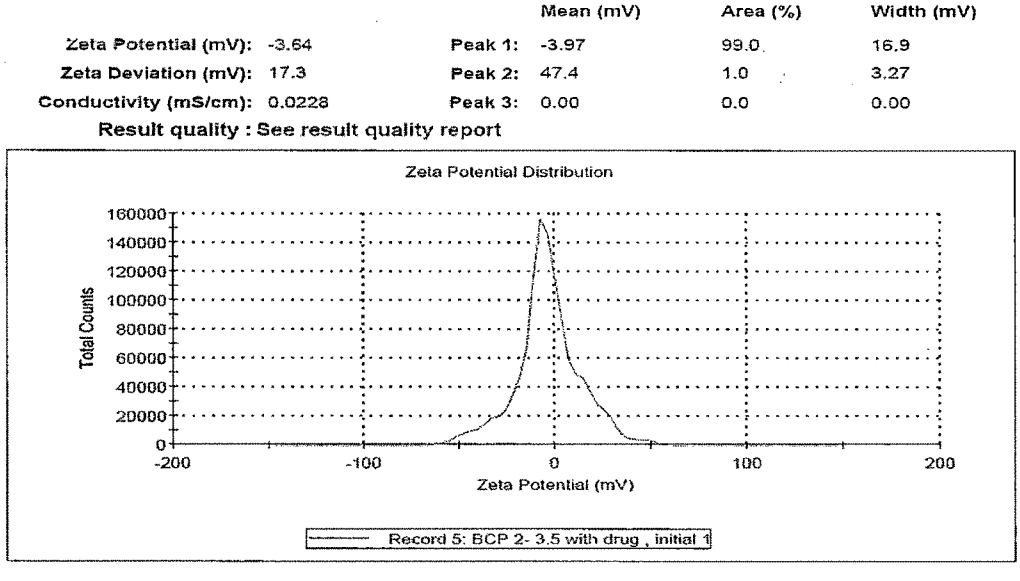

Figure 5.9 Zeta potential of ETO loaded MPCL 235 micelles

5.4.2.2 Critical micelle concentration

It is known that the stability of micelles both in vitro and in vivo depends on the CMC values. Upon dilution to CMC, micelles would begin to dissociate into unimers and thus release drugs. In general, lower the CMC value, better will be the micelle stability. To investigate the self-aggregation behavior of PEG-PCL block copolymers in an aqueous milieu, pyrene was used as a fluorescence probe because of its photophysical properties. Pyrene is strongly hydrophobic molecule with very low water solubility; moreover the fluorescence of the probe is sensitive to the change in the micro-environment, which permits monitoring of its incorporation in block copolymeric micelles at concentrations exceeding the CMC (Kim et al., 2005). Pyrene molecules preferentially accumulate into the hydrophobic microdomains of micelles rather than aqueous phase and shows different photophysical characteristics depending on the concentration of micelle forming materials as shown in Figure 5.10.

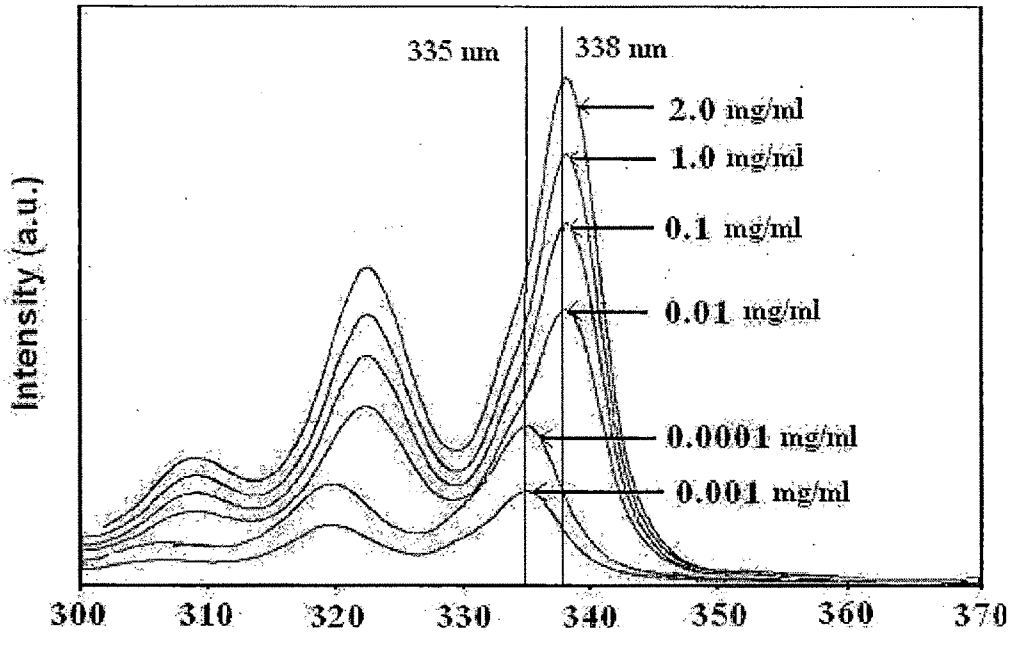

Figure 5.10 Excitation spectra of pyrene as a function of MPCL250 micelle concentration in water at room temperature

The CMC values were obtained from the self aggregation behaviors of the MPCL micelles in an aqueous phase using fluorescence emission spectra of the copolymer solutions with various concentrations in the presence of 6.0 X 10^{-7} M pyrene and the

results are illustrated in Figure 5.11 & 5.12. It was observed that the intensity values remained almost constant below the critical micelle concentration while a substantial increase in fluorescence after certain concentration called CMC, reflected incorporation of pyrene in the hydrophobic core of the polymeric micelles. In another way, a low concentration of MPCL micelles below CMC, the marker of pyrene was dissolved in a polar environment of water and fluorescence intensity of I_{338}/I_{335} was very low while in the presence of micelles, a hydrophobic micelle core solubilized pyrene and resulted in an increase of fluorescence intensity of I_{338}/I_{335}. Based on the intensity versus concentration data, the CMC values of various MPCL micellar formulations were calculated by the crossover point at low concentration ranges (Figure 5.11 and 5.12). The CMC values of MPCL micelles obtained were in the range of 2.00 X 10^{-3} to 1.14 X 10^{-3} mg/ml as shown in Table 5.11. It was observed that as the molecular weight of hydrophobic part increased, CMC value decreases, implies that the hydrophobic PCL blocks mainly affect the CMC. Moreover, the CMC values obtained are in agreement with the values reported earlier for MPEG-PCL micelles (Choi et al., 2006).

Micelles	CMC (mg/ml) x 10^{-3}
MPCL220	2.00
MPCL235	1.86
MPCL250	1.73
MPCL550	1.65
MPCL570	1.38
MPCL5100	1.14

Table 5.11 Critical micelle concentration (CMC) of various MPCL micelles (n= 3)

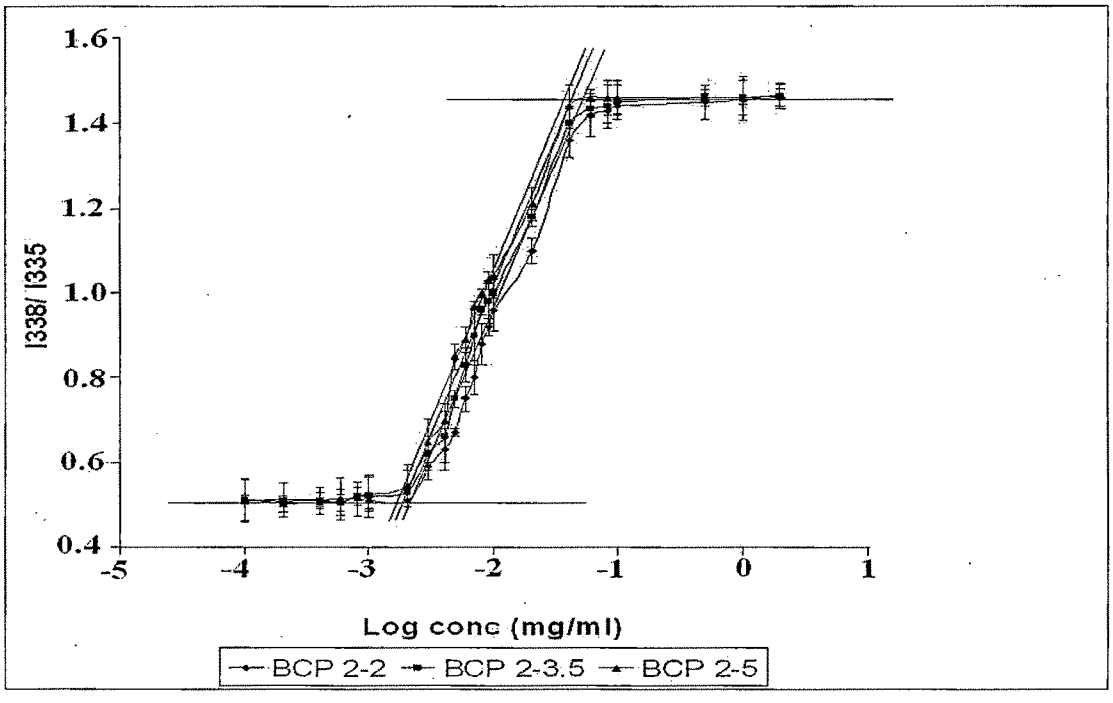

Figure 5.11 Plot of I_{338}/I_{335} (from pyrene excitation spectra) vs. log C for MPCL220, MPCL235 and MPCL250 micelles

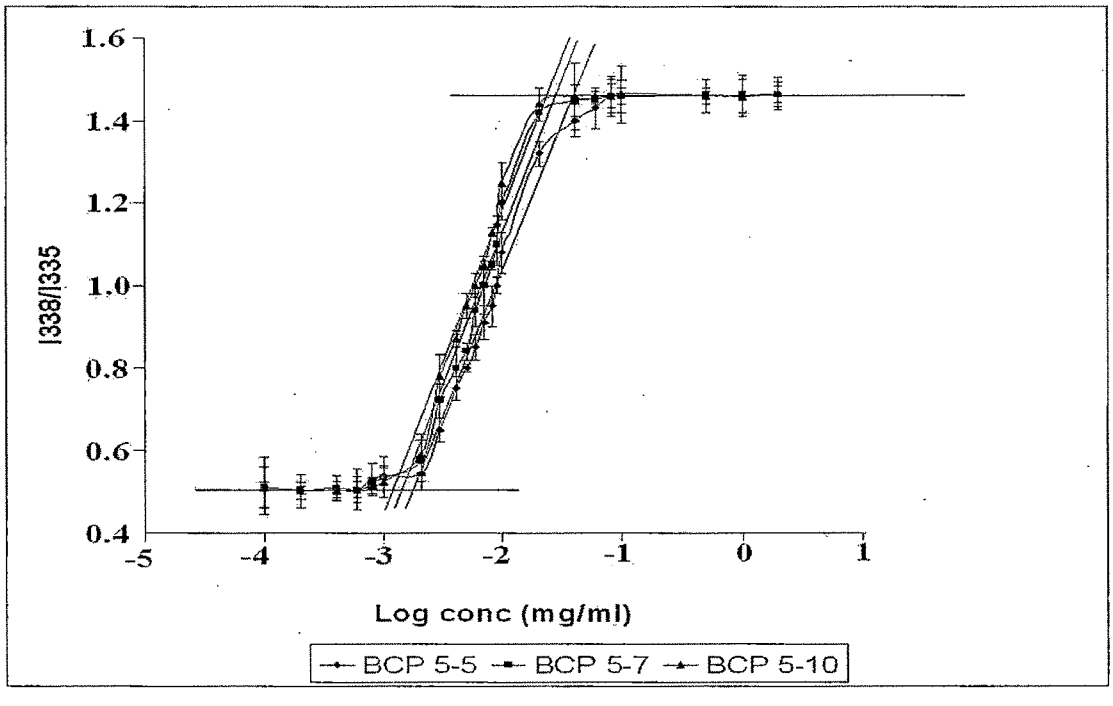

Figure 5.12 Plot of I_{338}/I_{335} (from pyrene excitation spectra) vs. log C for MPCL550, MPCL570 and MPCL5100 micelles

5.4.2.3 Fixed aqueous layer thickness

The *invitro* and *invivo* behavior of nanocarrier mainly depend on its particle size, zeta potential, PEG chain length and fixed aqueous layer thickness (Shai et al., 2005). Based on Gouy- Chapmann theory, the hydrodynamic drag caused by the PEG chains on the micelle surface moves the hydrodynamic plane of shear away from the charge-bearing plane and hence reduces the electrophoretic mobilities instead of the electrostatic surface potential (Shai et al., 2005). It is reported that a high negative zeta potential would facilitate the recognition of nanocarrier by the macrophages of the mononuclear phagocyte system (Gabizon & Papahedzopoulos, 1988) and therefore it is essential for the long-circulating micelles to have a less negative or even neutral zeta potential. It is supposed that when the concentration of the electrolyte was raised, the van der Waals attraction between the PCL core would exceed the surface charge repulsion. However, a high concentration of NaCl could also reduce the solvency power of water for PEG and resulting into flocculation of micelles (Avgoustakis et al., 2003). Hence, it is required that the concentration of NaCl should not exceed than 100 mM to prevent flocculation. Presence of PEG chain on the surface of micelle with formation of the fixed aqueous layers can prevent the attraction of opsonins; avoid the serum proteins binding and RES uptake (Sadzuka et al., 2002).

In this experiment, a rapid negativity reduction in charge of MPCL micelles with increasing NaCl concentration was elucidated quantitatively by measuring the fixed aqueous layer thickness (Table 5.12). It was found that upon increasing NaCl concentration, zeta potential of micelles decreased more prominently in micelles carrying PEG of molecular weight 5000. Moreover, micelles with PEG of mol wt 5000 exhibited higher thickness of aqueous layer compared to micelles carrying PEG of mol wt 2000. The results obtained are in confirmation with Shai et al. (2005). The FALT of MPCL micelles calculated based on Gouy–Chapmann theory is represented in Table 5.13 and Figure 5.13 & 5.14. ETO loaded micellar formulations exhibited less FALT value compared to placebo micellar formulations and it was assumed due to presence of drug (ETO) in core part of micelles, which might have altered the physicochemical properties of micelles surface like zeta potential and hydrophobic interaction between core part and drug. Similar findings were reported by Reddy &

Venkateswarlu (2005), who prepared parenteral emulsion using DSPE-PEG using ETO in which decrease of FALT value in presence of drug was observed.

Sample Code	Zeta potential of MPCL micelles after incubation with NaCl				
	Initial	25 mm	50 mm	75 mm	100 mm
MPCL220-P	-4.40 ± 0.23	-2.40 ± 0.35	-1.34 ± 0.12	-0.84 ± 0.31	-0.66 ± 0.27
MPCL220	-4.76 ± 0.65	-2.38 ± 0.21	-1.53 ± 0.24	-1.10 ± 0.20	-0.67 ± 0.18
MPCL235- P	-4.38 ± 0.45	-1.97 ± 0.30	-1.36 ± 0.14	-0.82 ± 0.22	-0.70 ± 0.10
MPCL235	-4.25 ± 0.28	-1.93 ± 0.24	-1.13 ± 0.38	-0.98 ± 0.14	-0.72 ± 0.16
MPCL250- P	-4.86 ± 0.35	-1.85 ± 0.38	-1.29 ± 0.34	-1.05 ± 0.25	-0.83 ± 0.22
MPCL250	-4.71 ± 0.38	-1.89 ± 0.45	-1.42 ± 0.33	-1.30 ± 0.35	-0.73 ± 0.31
MPCL550 -P	-4.80 ± 0.54	-0.82 ± 0.31	-0.56 ± 0.10	-0.39 ± 0.06	-0.27 ± 0.09
MPCL550	-4.66 ± 0.51	-0.84 ± 0.25	-0.51 ± 0.05	-0.43 ± 0.11	-0.33 ± 0.12
MPCL570 -P	-4.92 ± 0.48	-0.80 ± 0.10	-0.54 ± 0.09	-0.44 ± 0.09	-0.31 ± 0.05
MPCL570	-4.81 ± 0.40	-0.85 ± 0.15	-0.53 ± 0.11	-0.47 ± 0.07	-0.33 ± 0.11
MPCL5100-P	-4.61 ± 0.67	-0.87 ± 0.21	-0.57 ± 0.12	-0.46 ± 0.08	-0.32 ± 0.16
MPCL5100	-5.02 ± 0.61	-0.91 ± 0.23	-0.64 ± 0.08	-0.58 ± 0.06	-0.35 ± 0.14

Table 5.12 Zeta potentials of MPCL micelles in ionic solution containing various concentration of NaCl (The results are mean ± S.D. and n=3)

Formulation Code	FALT (nm)
MPCL220-P	3.35
MPCL220	3.25
MPCL235-P	3.22
MPCL235	3.05
MPCL250-P	3.04
MPCL250	2.94
MPCL550-P	4.88
MPCL550	4.69
MPCL570-P	4.71
MPCL570	4.56
MPCL5100-P	4.52
MPCL5100	4.40

Table 5.13 Fixed aqueous layer thickness (FALT) of ETO loaded and placebo MPCL micelles (Results are mean of three experiments)

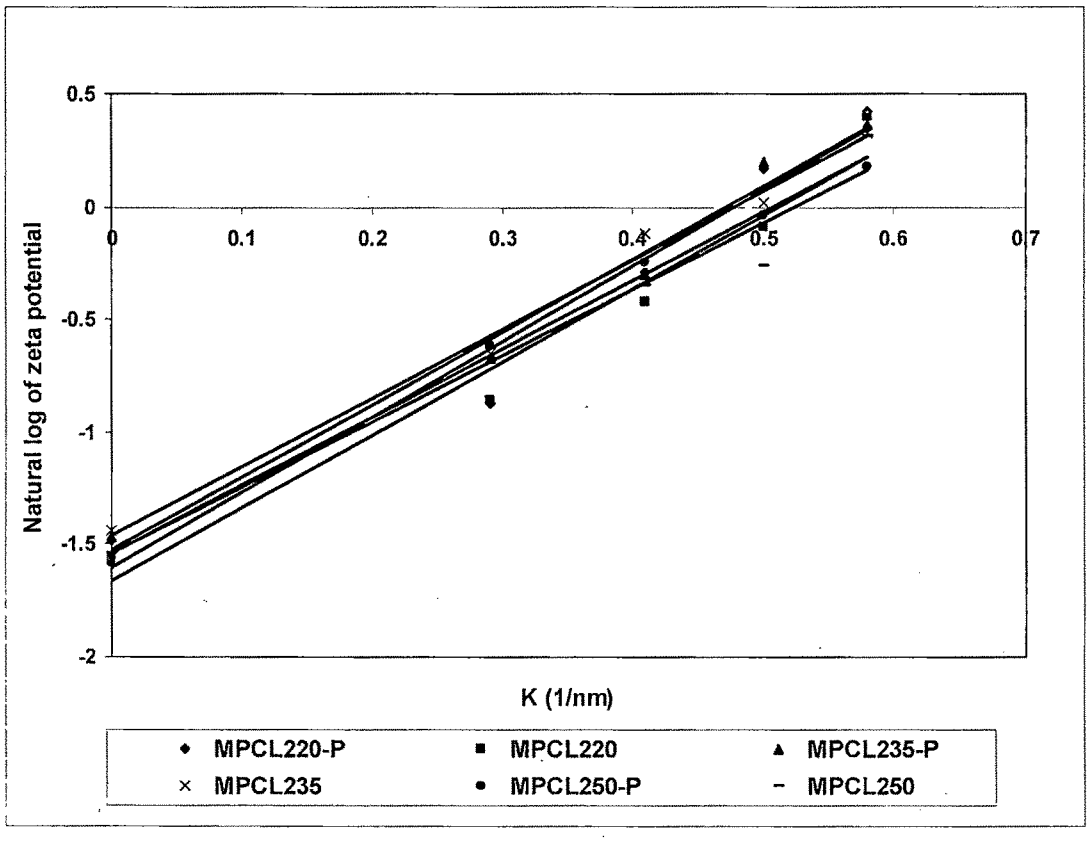

MPCL220-P	y= 3.3535x- 1.6038 R^2= 0.9617
MPCL220	y= 3.2504x- 1.6632 R^2= 0.9676
MPCL235-P	y= 3.2246x- 1.5239 R^2= 0.9853
MPCL235	y= 3.0542x- 1.4593 R^2= 0.9915
MPCL250-P	y= 3.0441x- 1.5437 R^2= 0.9958
MPCL250	y= 2.9422x- 1.5414 R^2= 0.9670

Figure 5.13 Natural log of zeta potential vs. K of MPCL220, MPCL235 and MPCL250 micelles with and without drug. Table at bottom represents the regressed equation for various formulations and slope m indicated the fixed aqueous layer thickness

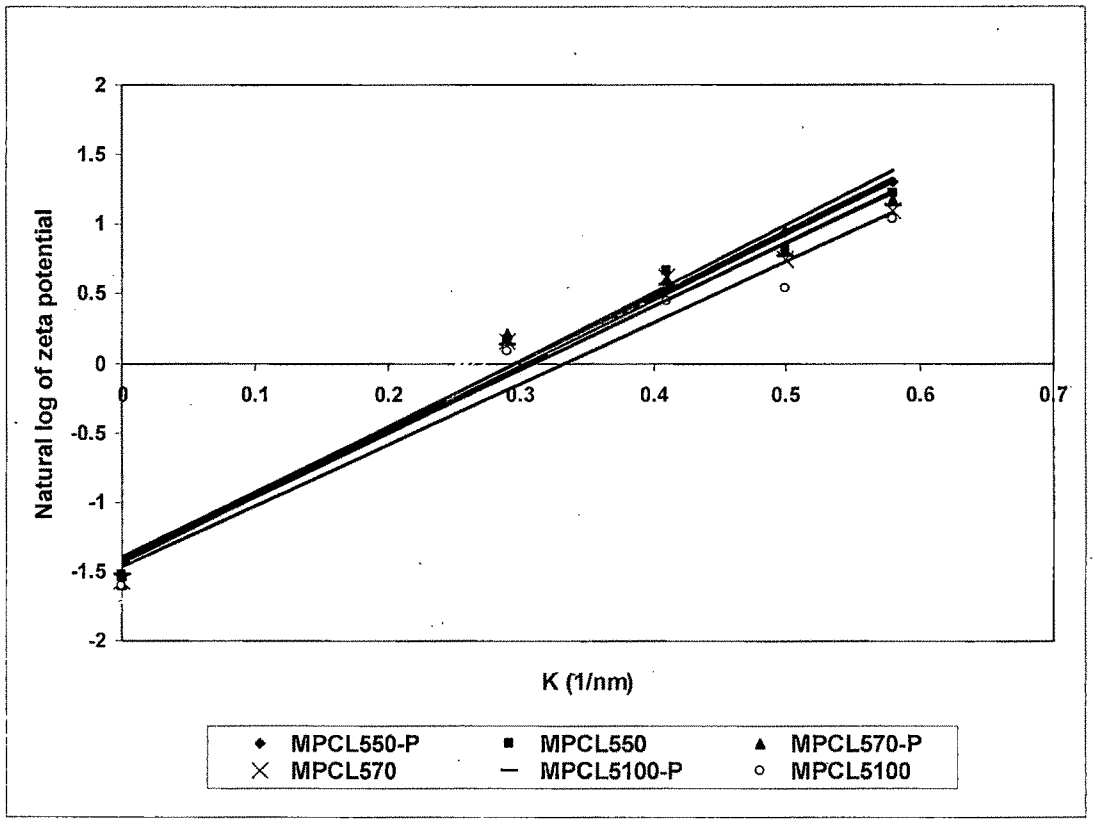

MPCL550-P	y= 4.8834x- 1.4485 R^2=0.9854
MPCL550	y= 4.6967x- 1.4000 R^2= 0.9771
MPCL570-P	y= 4.7182x- 1.4317 R^2= 0.9694
MPCL570	y= 4.5688x- 1.4145 R^2= 0.9672
MPCL5100-P	y= 4.5226x- 1.3961 R^2= 0.9789
MPCL5100	y= 4.4029x- 1.4654 R^2= 0.9633

Figure 5.14 Natural log of zeta potential vs. K of MPCL550, MPCL570 and MPCL5100 micelles with and without drug. Table at bottom represents the regressed equation for various formulations and slope m indicates the fixed aqueous layer thickness

5.4.2.4 *In vitro* stability studies

In vitro stability of MPCL micelles (with and without ETO loaded) was studied by measuring the particle size of micelles in the presence and absence of BSA in PBS pH 7.4 at various time point interval incubated at 37 °C. It has been postulated that interaction of serum protein is one of the key factor that concern the in vivo fate of systemic drug delivery vehicles such as liposomes and nanoparticles (Liu et al., 2005). Upon intravenous injection of nanocarrier, it is exposed to the vast group of proteins present within the bloodstream. Figure 5.15 represents two possible mechanisms by which protein may influence the in vivo behavior of micelles. In the first case, after intravenous administration opsonins/ proteins may adsorb on the surface of nanocarrier immediately which leads to opsonization and rapid clearance by RES system particularly if the surface is charged or hydrophobic (Ishihara et al., 1998). Secondly, if the drug has high protein affinity, drug might leach out rapidly due to attraction by proteins (Liu et al., 2005). The protein bound drug will likely be cleared more rapidly from the circulation without much accumulation at the tumor site, in comparison to vehicle-loaded drug (Nakanishi et al., 2001).

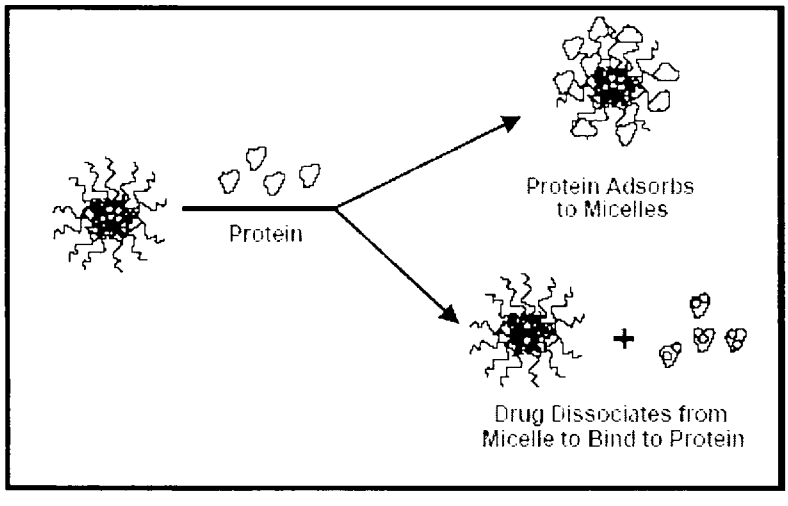

Figure 5.15 Influence of serum proteins on block copolymeric micelles as drug delivery systems

To avoid or reduce protein accumulation on the surface of nanocarrier, presence of PEG on the surface of nanocarrier is required. Very few studies have been carried out by group of Kabanov et al. (1995) and Liu et al. (2005 & 2007) for the adsorption of blood components using Pluronic-R triblock copolymer, PEG-PLA and PEG-PCL di-block copolymer. And they have observed that these carrier systems did not adsorb

significant quantities of blood protein and the presence of protein had not changed the size or sedimentation coefficient of the micelles. So, it is a matter of challenge for micelles to behave as true carriers rather than mere solubilizers, since the drug may have tendency to quickly release from the micelle following intravenous administration.

It was necessary to investigate the effect of protein on in vivo performance of various MPCL micelles. Moreover, ETO has been reported to have high protein affinity near to 95 % (Aita et al., 1999). Particle size analysis of micelles in the presence of total serum is not possible as some blood proteins (i.e. immunoglobulins) form aggregates in aqueous solution and hence bovine serum albumin (BSA) was used in this studies which is the most abundant plasma protein found in blood. MPCL micellar solution was incubated with equal volume of PBS (with and without presence of BSA [45 g/L]) and particle size was measured at different time interval. The particle size obtained is represented in Table 5.14 & 5.15. Placebo batches of MPCL micelles were also investigated to compare it with ETO loaded MPCL micelles.

Formulation Code		**Particle Size (nm)**				
	Incubation medium	**Initial**	**1 h**	**3 h**	**18 h**	**48 h**
MPCL220-P	PBS	36.15 ± 2.56	46.78	65.67	137.8	267.2
	PBS + BSA		43.76	68.61	145.2	301.7
MPCL220	PBS	38.32 ± 3.01	65.66	80.12	168.6	306.6
	PBS + BSA		73.90	90.55	176.9	326.7
MPCL235-P	PBS	38.67 ± 4.09	39.21	39.89	41.87	43.38
	PBS + BSA		39.28	40.31	42.43	44.62
MPCL235	PBS	39.54 ± 3.76	40.87	42.32	43.90	46.73
	PBS + BSA		40.66	42.78	44.55	48.46
MPCL250-P	PBS	51.34 ± 2.80	52.34	53.21	57.65	60.05
	PBS + BSA		53.45	56.09	59.50	64.31
MPCL250	PBS	53.65 ± 3.23	54.01	56.87	61.56	66.80
	PBS + BSA		54.43	59.96	63.94	69.49

Table 5.14 Influence on particle size of MPCL220, MPCL235 and MPCL250 micelles incubated with PBS in absence and presence of BSA (n=3)

Formulation Code	Incubation medium	Particle Size (nm) ± SD				
		Initial	1 h	3 h	18 h	48 h
MPCL550-P	PBS	65.78 ± 3.43	66.41	68.12	73.08	80.93
	PBS + BSA		67.09	68.95	76.60	82.53
MPCL550	PBS	67.21 ± 2.98	68.11	70.21	74.22	81.92
	PBS + BSA		68.40	72.52	77.91	82.95
MPCL570-P	PBS	72.76 ± 3.67	72.78	73.66	77.53	83.80
	PBS + BSA		73.01	75.14	79.29	84.31
MPCL570	PBS	74.54 ± 4.08	74.86	75.12	78.59	83.04
	PBS + BSA		75.91	76.81	79.58	85.06
MPCL5100-P	PBS	74.85 ± 3.31	75.48	76.85	80.69	85.24
	PBS + BSA		75.91	77.28	83.62	87.53
MPCL5100	PBS	76.56 ± 2.43	79.32	80.98	83.97	90.96
	PBS + BSA		78.34	81.56	87.09	91.20

Table 5.15 Influence on particle size of MPCL550, MPCL570 and MPCL5100 micelles incubated with PBS in absence and presence of BSA (n=3)

It was observed that all MPCL micelles remained stable after incubation in presence of and absence of BSA except MPCL220 and MPCL220-P micelles (Table 5.14 & 5.15) The particle size of MPCL 220-P and MPCL220 were increased from 36.15 nm and 38.32 nm to 267.2 and 306.6 nm respectively in absence of BSA at 48 h. At the same time in presence of BSA, particle size of both micelles was increased upto 301.7 nm and 326.7 nm. This indicates that MPCL220-P and MPCL220 micelles were not stable upon storage and resulting in to increase in particle size due to interaction with BSA. Moreover, the instability exerted by MPCL220 was higher compared to MPCL220-P micelles, which implies the interaction BSA with ETO resulted in to precipitation of drug which hampered the stability of micelles. The instability of MPCL220-P micelles was supposed be due to the reduction in population of unimers present in solution due to protein-polymer interaction which could result in to micelles dissociation.

The enhanced stability of micelles except MPCL220 and MPCL220-P even after 48 h of incubation indicates that stronger interaction exists between drug and core forming block which prevented the drug protein interactions (Figure 5.16 & 5.17). The results obtained suggest that BSA was adsorbed to minor extent on the surface of micelles and the finding are in agreement with previous report (Liu et al., 2005).

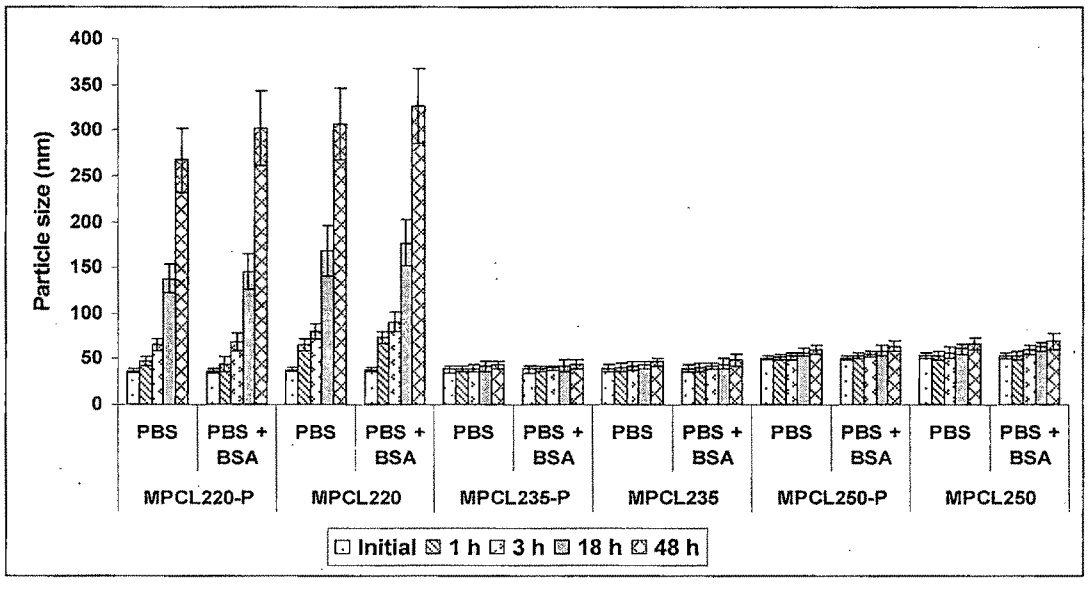

Figure 5.16 Effect on particle size of MPCL220, MPCL235 and MPCL250 micelles after incubation in presence and absence of BSA (n=3)

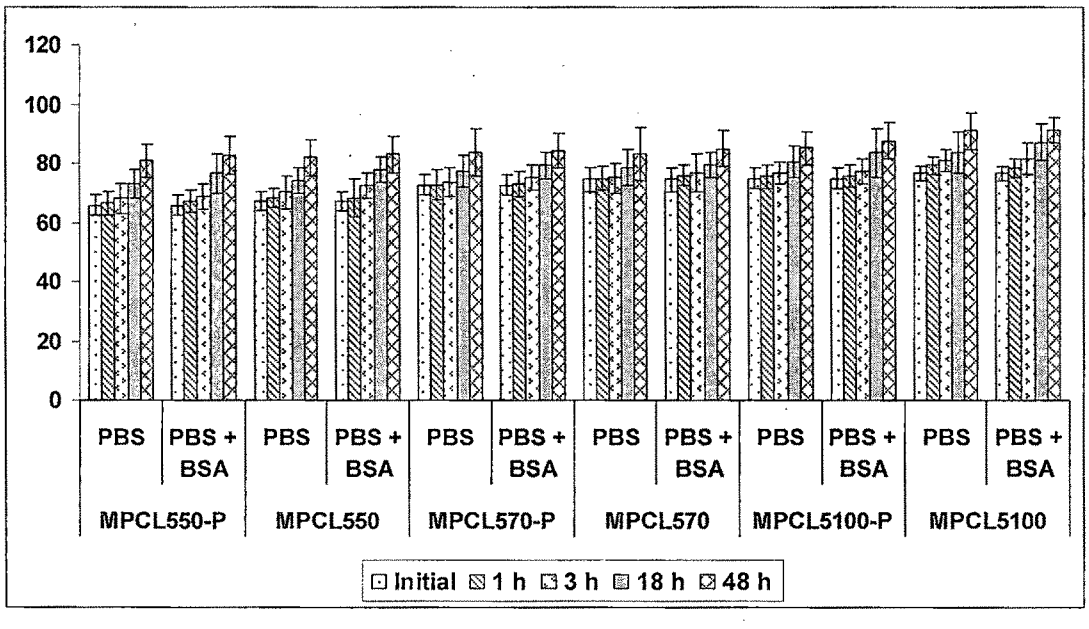

Figure 5.17 Effect on particle size of MPCL550, MPCL570 and MPCL5100 micelles after incubation in presence and absence of BSA (n=3)

5.4.2.5 PEG surface density

It is required that injected polymeric nanocarrier should not be recognized as foreign particles in body by RES system and to avoid this hydrophilic, flexible, non ionic polymers such as polyethylene glycol (PEG) is essential. PEG can give stealth properties to the injected particles, by preventing any interaction with blood proteins (opsonins) (Paracchia et al., 1997). PEG coating in polymeric nanoparticles reduced either protein adsorption or complementing activation and this dysopsonic effect was a function of PEG density, as reported for PEG-PLA nanoparticles by Vittaz et al. (1996). Similar findings were also observed by Jeon et al. (1991) in the study of protein surface interaction in the presence of PEO. They reported that high surface density and long chain length of PEO are desirable for protein resistance, although they observed that PEO surface density has a greater effect than chain length on the steric repulsion. Till date, most of the studies were performed with nanoparticles without drug and hence it is necessary to find out the effect of entrapped drug on PEG surface density and distance between two neighboring chain of PEG. The PEG surface density and average distance (nm) between two neighboring chain of PEG in MPCL micelles were investigated and the results obtained are represented in Table.5.16

It was observed that PEG surface density/nm^2 for MPCL220, MPCL235 and MPCL250 micelles were in between 0.830 to 0.753 with distance (D) from 1.20 to 1.33 nm. While MPCL550, MPCL570 and MPCL5100 micelles exhibited PEG surface density between 0.640 to 0.493 with distance (D) from 1.56 to 2.02 nm. Upon increasing the molecular weight of hydrophobic core, reduction in the surface density with increase in distance between two PEG chains was found. This might be because of strengthened hydrophobic interaction between PCL chain length, which occupied less molecular number of di-block copolymer to shape a single micelle. Moreover, the results obtained are in accordance with Shai et al. (2005), who observed similar phenomena in MPCL micelles loaded with drug hydrocamptothecin. Placebo MPCL micelles showed higher PEG surface density and lesser distance (D) between two PEG chains as compared to ETO loaded MPCL micelles. The possible explanation for these might be due to presence of drug on the surface of micelles which altered the density of PEG and distance (D) between two PEG chains.

Formulation code	Fraction of PEG (α)	PEG surface density/ nm^2 (δ)	Average distance (D) nm
MPCL220-P	0.457 ± 0.032	0.830	1.20
MPCL 220	0.442 ± 0.030	0.823	1.21
MPCL235-P	0.419 ± 0.021	0.802	1.24
MPCL235	0.405 ± 0.044	0.791	1.26
MPCL250-P	0.280 ± 0.052	0.753	1.33
MPCL250	0.278 ± 0.023	0.751	1.32
MPCL550-P	0.473 ± 0.031	0.640	1.56
MPCL550	0.459 ± 0.063	0.631	1.58
MPCL570-P	0.399 ± 0.040	0.585	1.70
MPCL570	0.385 ± 0.038	0.572	1.74
MPCL5100-P	0.338 ± 0.026	0.516	1.93
MPCL5100	0.320 ± 0.050	0.493	2.02

D is the average distance D between two neighboring PEG

Table 5.16 PEG surface density and average distance (nm) between two neighboring chain of MPCL micelles (Results are mean of three experiments)

A decrease in surface density with increased in distance (D) in MPCL micelles carrying PEG of mol wt 5000 was seen compared to MPCL micelles carrying PEG 2000. PEG was reported to change the association of the copolymer molecules during the formation of the particles (Riley et al., 1999). Thus, it could be predictable that longer PEG chain require more space to retain their flexibility, which made the surface PEG sparser. It was studied by Gref et al. (2000), that flexibility of the PEG is depend on its chain length which is essential to escape the cells of the mononuclear phagocyte system. They also observed that a certain range of PEG surface density was also needed for maintaining its flexibility. Furthermore, Bazile et al. (1995) suggested that a distance of 1.2–1.4 nm between two grafted PEG 2000 chains is required for avoiding complement consumption while Jeon et al., (1991) recommended that distance between two PEG chain should be around 1 nm to avoid the adsorption of small proteins (approximated as spheres with a radius of 2 nm) and around 1.5 nm for larger proteins (6-8 nm). These values could be very helpful to understand the *in vivo* behavior of the MPCL micelles.

5.4.2.6 Hemolysis study

Erythrocytes are among the first cells that come into contact with foreign materials in the blood system. Hemolysis (destruction of red blood cells) in vivo can lead to anemia, jaundice, and other pathological conditions; therefore the hemolytic potential of all intravenously administered pharmaceuticals must be evaluated during preclinical studies (Jumaa & Muller, 1999; Amin & Dannenfelser, 2006). It is well known that surfactants at high concentration are capable of disrupting cell membranes, such as those of erythrocytes by penetration and saturation of the membrane with unimers followed by solubilization of the membrane lipids and proteins (Letchford et al., 2009).

The *in vitro* hemolysis study was performed with various concentrations of drug loaded MPCL micelles. ETO injection and placebo ETO injection were also evaluated to check the hemolysis effect of free drug and excipients respectively. The dose of ETO injection is 50 to 100 mg/M^2 per day and based on the surface area of body the average dose of ETO for adult is 130 mg/day and accordingly concentration of ETO in blood on single dose will remains around 20 µg/ml. Although, the hemolytic studies were carried out upto concentration range of 200 µg/ml to know the immediate effect ETO concentration on hemolysis when it comes in contact with erythrocytes. ETO injection showed hemolysis of 29.82 ± 4.34 percent at concentration of 25 µg/ml while placebo ETO formulation at similar concentration showed percent hemolysis of 5.88 ± 2.65 (Table 5.17 & Figure 5.18). This implies that marketed product of ETO injections has substantial hemolytic properties, at the same time placebo injection also showed hemolytic properties because of surfactant like tween-80, PEG-300 etc. Compared to plain ETO, all micellar formulations showed very less hemolytic potential after 30 min of incubation.

MPCL micellar formulations except MPCL220 showed very less or negligible hemolytic effect even after 24 h of incubation (Table 5.17 and Figure 5.18 & 5.19). The percent hemolysis after 24 h of incubation was between 1 to 5 % at ETO concentration of 200 µg/ml in all MPCL micelles except MPCL220. A significant hemolysis with MPCL220 was observed compared to other MPCL micellar formulation and this result was attributed to rapid release of drug from micelles due to its lower molecular weight. Zastre et al. (2007) observed similar findings with short

block length copolymer which was capable of inducing rapid and significant hemolysis. Due to presence of hydrated state of PEG on the surface of micelles with stable core, the micelles would remain intact; however few available unimers may likely to penetrate in to cell membrane and resulting in to hemolysis (Letchford et al., 2009).

Formulation Code	ETO concentration (µg/ml)	Time of incubation		
		30 min	4 h	24 h
		% Hemolysis (Mean ± S.D)		
Etoposide Injection	200	92.28 ± 5.78	N.D.	N.D.
	100	61.40 ± 4.64	N.D.	N.D.
	50	54.38 ± 5.08	N.D.	N.D.
	25	29.82 ± 4.34	N.D.	N.D.
Placebo Inj. (ETO)	200*	42.64 ± 6.54	N.D.	N.D.
	100*	27.94 ± 3.90	N.D.	N.D.
	50*	14.70 ± 3.71	N.D.	N.D.
	25*	5.88 ± 2.65	N.D.	N.D.
MPCL220	200	2.43 ± 0.92	7.19 ± 2.90	20.0 ± 4.57
	100	1.01. ± 0.78	5.00 ± 1.65	11.56 ± 2.08
	50	0.70 ± 0.23	2.54 ± 1.89	7.58 ± 3.56
	25	0.32 ± 0.19	0.87 ± 0.34	5.32 ± 2.43
MPCL235	200	1.55 ± 0.77	3.50 ± 1.09	5.60 ± 2.87
	100	0.60 ± 0.31	1.33 ± 0.51	4.0 ± 1.98
	50	0.40 ± 0.22	0.70 ± 0.21	2.03 ± 0.68
	25	0.30 ± 0.08	0.65 ± 0.17	1.67 ± 0.79
MPCL250	200	0.87 ± 0.21	1. 60 ± 0.89	2.61 ± 0.80
	100	0.65 ± 0.45	1.21 ± 0.56	1.67 ± 0.77
	50	0.54 ± 0.43	0.98 ± 0.65	1.32 ± 0.84
	25	0.24 ± 0.11	0.43 ± 0.30	0.65 ± 0.23
MPCL550	200	1.11 ± 0.76	2.56 ± 0.91	3.31 ± 1.29
	100	0.67 ± 0.23	1.34 ± 0.76	2.98 ± 1.01
	50	0.55 ± 0.31	1.03 ± 0.65	2.02 ± 0.78
	25	0.30 ± 0.19	0.58 ± 0.40	0.90 ± 0.15
MPCL570	200	1.02 ± 0.32	2.19 ± 0.20	3.08 ± 0.99
	100	0.63 ± 0.33	1.22 ± 0.56	2.76 ± 1.02
	50	0.53 ± 0.29	0.97 ± 0.61	1.87 ± 0.76
	25	0.44 ± 0.30	0.55 ± 0.25	1.02 ± 0.19
MPCL5100	200	1.00 ± 0.22	1.67 ± 0.20	2.10 ± 0.77
	100	0.61 ± 0.11	1.10 ± 0.24	1.89 ± 0.43
	50	0.51 ± 0.15	0.87 ± 0.18	1.55 ± 0.88
	25	0.21 ± 0.12	0.57 ± 0.21	0.87 ± 0.30

* Amount of Placebo injection of ETO added similar to ETO injection

Table 5.17 Effect of ETO injection and ETO loaded micelles on the hemolytic effect after incubation with erythrocyte at different time interval (n=3)

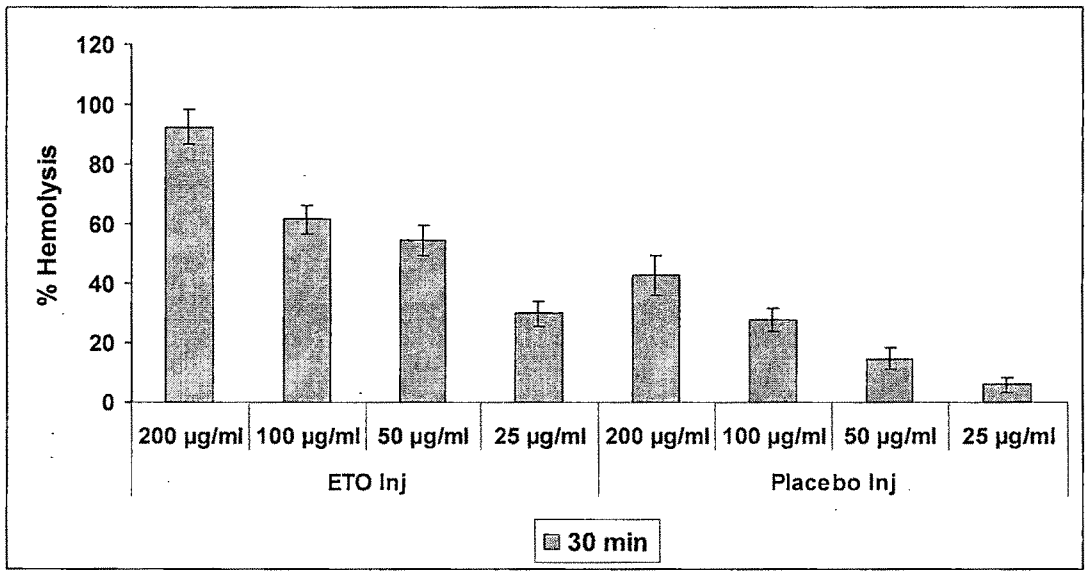

Figure 5.18 Percent hemolysis ETO injection and placebo injections (ETO) after 30 min of incubation with erythrocyte dispersion

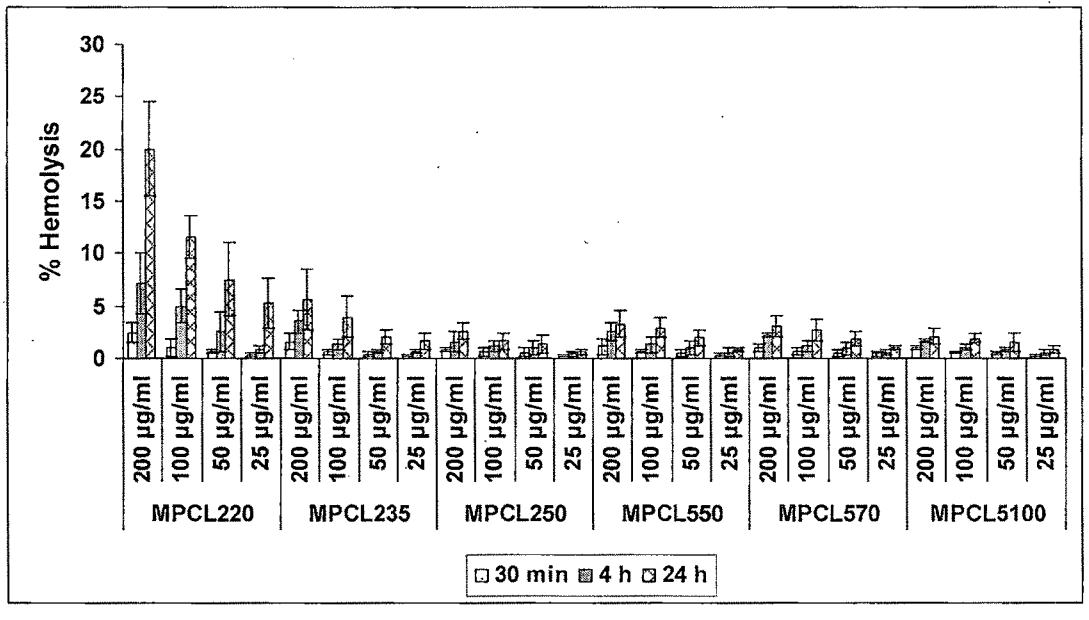

Figure 5.19 Percent hemolysis MPCL micelles after 30 min, 4 h and 24 h of incubation with erythrocyte dispersion

A hemolytic study of liposomal formulation of ETO performed by Khan et al. (2007) also reported that liposomal formulation has less toxicity compared to free ETO. Similar studies were also carried out on block copolymeric micellar system containing various anticancer drug and it was observed that block copolymeric nanocarrier are safe and having negligible hemolytic activities (Shaui et al., 2004a, Letchford et al.,

2009). The study suggests that the use of nanocarrier is very much effective in reducing hemolysis activities of drug with avoidance of use of vehicle responsible for hemolysis.

5.5 SELECTION OF MPCL MICELLES

It was required to select the two MPCL micellar formulations for further studies like peptide conjugation, invitro and in vivo studies. Two MPCL micellar formulations were selected with one from micelles carrying PEG of mol wt 2000 i.e. MPCL235 and other from micelles with PEG mol wt 5000 i.e.MPCL570 based on their particle size, percent entrapment and PDI. Moreover, critical micelle concentration (CMC), PEG surface density, fixed aqueous layer thickness (FALT), in vitro stability and hemolytic studies results were also taken in account for selection of MPCL micelles. MPCL220 micellar formulation was rejected on the base of their poor performance exhibited in various studies as mentioned earlier. MPCL235 and MPCL250 micelles showed acceptable outputs with related to their drug loading and particle size based on their molecular weight but the PDI was found lesser in MPCL235 compared to MPCL250 micelles and hence MPCL235 micelles was used for further studies. MPCL550, MPCL570 and MPCL5100 micelles showed comparable results for particle size, PDI and percent drug loading with respect to the molecular weight of copolymer used. The hemolytic effect, FALT, PEG surface density and invitro stability studies showed agreeable results for MPCL550, MPCL570 and MPCL5100 micelles, which made difficult for selection of MPCL micellar formulation but based on the comparative results MPCL570 was selected for further studies.

Based on selection of two MPCL micelles i.e. MPCL235 and MPCL570, two functionalized di-block copolymer HOOC-PEG-PCL i.e. FBCP 2-3.5 and FBCP 5-7 of molecular weight similar to BCP 2-3.5 and BCP 5-7 were synthesized and characterized as reported in chapter 4.0.

REFERENCES

Aita P, Robieux I, Tumolo RS, Cannizzaro CR, Boiocchi AM, Toffoli G. Pharmacokinetics of oral etoposide in patients with hepatocellular carcinoma. Cancer Chemother Pharmacol 1999; 43: 287-294.

Aliabadi HM, Mahmud A, Dehmoobed SA, Lavasanifar A. Micelles of methoxy poly(ethylene oxide)-*b*-poly(_-caprolactone) as vehicles for the solubilization and controlled delivery of cyclosporine A. J Control Release 2005; 104: 301–311.

Aliabadi HM, Elhasi S, Mahmud A, Gulamhusein R, Mahdipoor P, Lavasanifar A. Encapsulation of hydrophobic drugs in polymeric micelles through co-solvent evaporation: The effect of solvent composition on micellar properties and drug loading. Int J Pharm 2007; 329: 158-165.

Allen C, Han J, Yu Y, Maysinger D, Eisenberg A. Polycaprolactone-*b*- poly(ethylene oxide) copolymer micelles as a delivery vehicle for dihydrotestosterone. J Control Release 2000; 63: 275–286.

Allen C, Maysinger D, Eisenberg A. Nano-engineering block copolymer aggregates for drug delivery. Colloids Surf B Biointerfaces 1999; 16: 3 – 27.

Allen C, Santos ND, Gallagher R, Chiu GNC, Shu Y, Li, WM, Johnstone SA, Janoff AS, Mayer LD, Webb MS, Bally MB. Controlling the physical behavior and biological performance of liposome formulations through use of surface grafted poly(ethylene glycol). Biosci Rep 2002; 22: 225– 250.

Amin K, Dannenfelser RM. In Vitro Hemolysis: Guidance for the Pharmaceutical Scientist. J Pharma Sci 2006; 95: 1173–1176.

Avgoustakis K, Belestsi A, Panagi Z, Klepetsanis P, Livaniou E, Evangelatos G, Ithakissios DS. Effect of copolymer composition on the physicochemical characteristics, in vitro stability and biodistribution of PLGA-mPEG nanoparticles. Int J Pharm 2003; 259:115-127.

Bazile D, Prud'Homme C, Bassoulet MT, Marlard M, Spenlehauer G, Veillard M. Stealth Me.PEG-PLA nanoparticles avoid uptake by the mononuclear phagocytes system. J Pharm Sci 1995; 84:493-498.

Choi C, Chae SY, Kim TH, Kweon JK, Cho CS, Jang MK, Nah JW. Synthesis and physicochemical characterization of amphiphilic block copolymer self-aggregates formed by poly(ethylene glycol)-*block*-poly(ε-caprolactone). J Applied Polymer Sci 2006; 99: 3520–3527.

Gabizon A, Papahedzopoulos D. Liposome formulations with prolonged circulation time in blood and enhanced uptake by tumors. Proc Natl Acad Sci USA 1988; 85: 6949-6953.

Gadelle F, Koros WJ, Schechter RS. Solubilization of aromatic solutes in block copolymers. Macromolecules 1995; 28: 4883-4892.

Gan Z, Jim TF, Li M, Yuer Z, Wang S, Wu C. Enzymatic biodegradation of poy(ethylene oxide-b-e-caprolactone) diblock copolymer and its potential biomedical applications.. Macromolecules 1999; 32: 590-594.

Gref R, Luck M, Quellec P, Marchand M, Dellacherie E, Harnisch S, Blunk T, Muller RH. 'Stealth' corona-core nanoparticles surface modified by polyethylene glycol (PEG): influences of the corona (PEG chain length and surface density) and of the core composition on phagocytic uptake and plasma protein adsorption. Coll Surf B Biointerf 2000; 18: 301–313.

Hu Y, Xie J, Tong YW, Wang CH. Effect of PEG conformation and particle size on the cellular uptake efficiency of nanoparticles with the HepG2 cells, J Control Release 2007; 118:7–17.

Ishihara K, Nomura H, Mihara T, Kurita K, Iwasaki Y, Nakabayashi N. Why do phospholipid polymers reduce protein adsorption? J Biomed Mater Res 1998; 39: 323–330.

Jeon SI, Lee JH, Andrade JD, De Gennes PG. Protein-surface interaction in the presence of polyethylene oxide. J colloid interface Science 1991; 142: 149-158.

Jette KK, Law D, Schmitt EA, Kwon GS. Preparation and drug loading of poly(ethylene glycol)-block-poly(epsilon-caprolactone) micelles through the evaporation of a co-solvent azeotrope. Pharm Res 2004; 21: 1184–1191.

Johnson BK, Prud'homme RK. Mechanism for rapid self assembly of block copolymer nanoparticles. Phys Rev Lett 2003a; 91:118302–118304.

Johnson, BK, Prud'homme RK. Flash nanoprecipitation of organic actives and block copolymers using a confined impinging jets mixer. Aust J Chem 2003b; 56: 1021–1024.
Jumaa M, Muller BW. In vitro investigation of the effect of various isotonic substances in parenteral emulsions on human erythrocytes. Eur J Pharm Sci 1999; 9: 207-212.

Kabanov AV, Nazarova IR, Astafieva IV, Batrakova EV, Alakhov VY, Yaroslavov AA Kabanov VA. Micelle formation and solubilization of fluorescent-probes in poly(oxyethylene-b-oxypropylene-b-oxyethylene) solutions. Macromolecules 1995; 28: 2303-2314.

Khan A, Khan AA, Dwivedi V, Ahmad MG, Hakeem S, Owais M. Tuftsin augments antitumor efficacy of liposomized etoposide against fibrosarcoma in swiss albino mice. Mol Med 2007; 13: 266-276.

Kim MS, Hyun H, Cho YH, Seo KS, Jang WY, Kim SK, Khang G, Lee HB. Preparation of methoxy poly(ethylene glycol)-block poly(caprolactone) via activated monomer mechanism and examination of micellar characterization. Pol Bull 2005; 55: 149–156.

Kim SY, Shin IG, Lee YM, Cho CS, Sung YK. Methoxy poly(ethylene glycol) and epsilon-caprolactone amphiphilic block copolymeric micelle containing indomethacin II. Micelle formation and drug release behaviors. J Control Release 1998; 51: 13–22.

Kim SY, Lee YM. Taxol-loaded block copolymer nanospheres composed of methoxy poly(ethylene glycol) and poly(ε-caprolactone) as novel anticancer drug carriers. Biomaterials 2001; 22: 1697-1704.

Kozlov MY, Melik-Nubarov NS, Batrakova EV, Kabanov AV. Relationship between pluronic block copolymer structure, critical micellization concentration and partitioning coefficients of low molecular mass solutes. Macromolecules 2000; 33: 3305-3313.

Letchford K, Liggins R, Wasan KM Burt H. In vitro human plasma distribution of nanoparticulate paclitaxel is dependent on the physicochemical properties of poly(ethylene glycol)-block-poly(caprolactone) nanoparticles. Eur J Pharm Biopharm 2009; 71:196–206.

Liu J, Zeng F, Allen C. Influence of serum protein on polycarbonate-based copolymer micelles as a delivery system for a hydrophobic anti-cancer agent. J Control Release 2005; 103: 481-497.

Liu J, Zeng F, Allen C. In vivo fate of unimers and micelles of a poly(ethylene glycol)-block-poly(caprolactone) copolymer in mice following intravenous administration. Eur J Pharm Biopharm 2007; 65: 309–319.

Moghimi SM, Pavey KD, Hunter AC. Real-time evidence of surface modification at polystyrene lattices by poloxamine 908 in the presence of serum: in vivo conversion of macrophage- prone nanoparticles to stealth entities by poloxamine 908. FEBS Lett 2003; 547: 177– 182.

Nakanishi T, Fukushima S, Okamoto K, Suzuki M, Matsumura Y, Yokoyama M, Okano T, Sakurai Y, Kataoka K. Development of the polymer micelle carrier system for doxorubicin, J Control Release 2001; 74: 295- 302.

Paracchia MT, Vauthier C, Passiranin C, Couvreur P, Labarre D. Complement consumption by poly(ethylene glycol) in different conformation chemically coupled to poly(isobutyl 2-cyanoacrylate) nanoparticles. Life Sci 1997; 61: 749- 761.

Patel HM, Moghimi SM. Serum-mediated recognition of liposomes by phagocytic cells of the reticuloendothelial system- the concept of tissue specificity. Adv Drug Deliv Rev 1998; 32: 45- 60.

Radek S, Mariusz U, Pavel M, Karel P, Miroslav S. Preparation and characterization of self-assembled nanoparticles formed by poly(ethylene oxide)-*block*-poly(ε-caprolactone) copolymers with long poly(ε-caprolactone) blocks in aqueous solutions. Langmuir 2007; 23: 3395-3400.

Reddy PR, Venkateswarlu V. Pharmacokinetics and tissue distribution of etoposide delivered in long circulating parenteral emulsion. J Drug Target 2005; 13: 543–553

Riley T, Govender T, Stolnik S, Xiong CD, Garnett MC, Illum L, Davis SS. Colloidal stability and drug incorporation aspects of micellar-like PLA–PEG nanoparticles. Coll Surf B 1999; 16: 147-159.

Sadzuka Y, Nakade A, Hirama R, Miyagishima A, Nozawa Y, Hirota S, Sonobe T. Effects of mixed polyethylene glycol modification on fixed aqueous layer thickness and antitumor activity of doxorubicin containing liposome. Int J Pharm 2002; 238: 171–180.

Shai B, Fang C, You MX, Zhang Y, Fu S, Pei YY. Stealth MePEG-PCL micelles: effects of polymer composition on micelle physicochemical characteristics, in vitro drug release, in vivo pharmacokinetics in rats and biodistribution in S180 tumor bearing mice. Colloid Polym Sci 2005; 283: 954–967.

Shuai, X, Ai H, Nasongkla N, Kim S, Gao J.. Micellar carriers based on block copolymers of poly(epsilon-caprolactone) and poly(ethylene glycol) for doxorubicin delivery. J Control Release 2004a; 98: 415–426.

Shuai X, Merdan T, Schaper AK, Xi F, Kissel T.. Core-cross-linked polymeric micelles as paclitaxel carriers. Bioconjug Chem 2004b; 15: 441–448.

Soppimath KS, Aminabhavi TM, Kulkarni AR, Rudzinski WE. Biodegradable polymeric nanoparticles as drug delivery devices. J of Control Release 2001; 70:1–20.

Tanodekaew S, Pannu R, Heatley F, Attwood D, Booth C. Association and surface properties of diblock copolymers of ethylene oxide and DL-lactide in aqueous solution. Macromol Chem Phys 1997; 198: 927-944.

Vangeyte P, Gautier S, Jerome R. About the methods of preparation of poly(ethylene oxide)-*b*-poly(ε-caprolactone) nanoparticles in water analysis by dynamic light scattering. Colloids Surf. A: Physiochem Eng Aspects 2004; 242: 203–211.

Vittaz M, Bazile D, Spenlehauer G, Verrecchia T, Veillard M, Puisieux F, Labarre D. Effect of PEO surface density on long circulating PLA-PEO nanoparticles which are very low complement activators. Biomaterials 1996; 17: 1575-1561.

Zastre J, Jackson JK, Wong W, Burt HM. Methoxypolyethylene glycol-block polycaprolactone diblock copolymers reduce P-glycoprotein efflux in the absence of a membrane fluidization effect while stimulating P-glycoprotein ATPase activity. J Pharm Sci 2007; 96: 864-875.

Zhang L, Hu Y, Jiang X, Yang C, Lu W, Yang YH. Camptothecin derivative-loaded poly(caprolactone-co-lactide)b-PEG-b-poly(caprolactone-co-lactide) nanoparticles and their biodistribution in mice. J Control Release 2004; 96: 135-148.

Zhang L, Allen C, Yu Y, Yu K, Bartels C, Shen H, Maysinger D, Eisenberg A. Nanoengineered aggregates of various architectures by controlled self-assembly of asymmetric amphiphilic diblock copolymers in solution. Polym Prepr (am chem soc div polym chem) 1998; 39:170-171.